Environmental Science
Water Research & Technology

PAPER

Cite this: *Environ. Sci.: Water Res. Technol.*, 2022, **8**, 543

Reactivities of hydrated electrons with organic compounds in aqueous-phase advanced reduction processes†

Rose Daily and Daisuke Minakata *

Advanced reduction processes (ARPs) that generate reactive electrons in homogeneous solution and heterogeneous electrochemical or catalytic processes are effective in degrading oxidized forms of organic and inorganic contaminants. However, the detailed mechanisms of compounds with multiple functional groups and the effect of those functional groups on the reactivities of these compounds toward electrons have not been elucidated. In this study, we use density functional theory to calculate the aqueous-phase one electron reduction potential $E^{\circ}_{red,aq}$ of 251 conventional organic compounds containing a wide variety of functional groups. We investigate three possible elementary reaction mechanisms, namely, the associative, concerted and stepwise cleavage mechanisms, at all possible reactive sites and determine the linear free energy relationships (LFERs) between the experimentally measured rate constants of hydrated electrons (e_{aq}^-) and the $E^{\circ}_{red,aq}$ values. In addition, we use the 75 priority per- and polyfluoroalkyl substance (PFAS) subsets from the United States Environmental Protection Agency (U.S. EPA) to calculate the $E^{\circ}_{red,aq}$ values of all possible elementary reactions of each PFAS to determine their dominant reaction mechanisms and reactive sites. LFERs of conventional organic compounds are used to predict the reactivities of e_{aq}^- with PFASs, which can be used as a screening tool to evaluate the electron-induced degradability of thousands of PFASs for both homogeneous and heterogeneous reduction processes. Finally, we develop a kinetic model to investigate the impact of an accurate rate constant prediction on the fate of an environmentally relevant organic compound induced by e_{aq}^- in a homogeneous aqueous-phase ARP.

Received 3rd December 2021,
Accepted 28th January 2022

DOI: 10.1039/d1ew00897h

rsc.li/es-water

Water impact

Oxidized forms of trace chemical contaminants including per- and poly-fluoroalkyl substances (PFAS) are the group of contaminants of emerging concern. Understanding and predicting the reactivity of solvated electrons enables prediction of the fate of contaminants in the aqueous-phase advanced reduction processes. A computational tool can be used to screen a number of contaminants to prioritize for the reduction processes.

Introduction

Free radical-based technologies are attractive and promising processes for destroying a wide variety of organic contaminants. Advanced oxidation processes (AOPs) that generate highly reactive oxygenated radical species (*e.g.*, hydroxyl radicals)[1,2] and other reactive radicals (*e.g.*, chlorine-,[3,4] bromine-[5] and nitrogen-derived radicals[6,7] and carbonate radicals[8]) at ambient temperature and atmospheric pressure have been proven to degrade reduced forms of organic contaminants in water at full-scale treatment plants. Advanced reduction processes (ARPs) that generate reactive radicals (*e.g.*, superoxide anion radicals) and electrons in homogeneous solution[9,10] and heterogeneous electrochemical[11–13] or catalytic[14] processes are effective in degrading the oxidized forms of organic and inorganic contaminants. Homogeneous, electrochemical, and a combination of both ARPs have been successfully applied for the degradation of conventional organic contaminants such as alkyl halides and emerging groups of contaminants such as per- and polyfluorinated alkyl substances (PFASs).[15]

While the reactivities of reactive radical species in AOPs have been actively studied and some predictive approaches

Department of Civil, Environmental, and Geospatial Engineering, Michigan Technological University, 1400 Townsend Drive, Houghton, MI, 49931, USA. E-mail: dminakat@mtu.edu; Fax: +1 906 487 2943; Tel: +1 906 487 1830

† Electronic supplementary information (ESI) available: Additional information for 4 text, 7 tables and 24 figures is available in the ESI1 as well as all *z*-matrix and optimized molecular and radical structures in the ESI2. See DOI: 10.1039/d1ew00897h

have been reported in the literature,[16] few studies have holistically focused on the reactivities of electrons in aqueous-phase ARPs. The reactivities of aqueous-phase hydrated electrons, e_{aq}^-, with a wide variety of individual organic compounds have been experimentally measured, and the second-order rate constants, k_{exp}, have been reported and compiled in the database[17] (see Fig. S1 in the ESI† for a box plot of k_{exp} values). However, few studies have developed a predictive tool for the k_{exp} values of e_{aq}^- due to a lack of mechanistic understanding of the reactivities with organic compounds.[18,19] In general, nucleophilic electrons react at the electron-deficient sites of organic compounds. The three major reaction mechanisms include (1) association with the π bond of a double bond; (2) concerted dissociative cleavage of a carbon halogen (C–X where X = F, Cl, Br or I) bond of haloalkanes or carbon–nitrogen (C–N) bond; and (3) stepwise cleavage of a C–X bond of haloalkanes and haloalkenes, a sulfur–sulfur (S–S) bond or a carbon–sulfur (C–S) bond of sulfides or disulfides.[20] Each reaction mechanism depends on the molecular structures and functional groups present in the same molecule. The overall reactivities with e_{aq}^- are reduced by electron-donating functional groups and increased by electron-withdrawing functional groups. However, the detailed mechanisms of multiple functional group compounds and the effect of these functional groups on the major reactivities have not been elucidated because of the difficulties in experimental investigations.

The use of quantum mechanics-based methods such as *ab initio* calculations or density functional theory (DFT) can complement experimental observations of chemical reactivities and provide mechanistic insight into reaction mechanisms. Several DFT-based methods were used to investigate the thermodynamics and kinetics of electron-induced reactions with halogenated compounds such as polychlorinated ethylenes,[21,22] polybrominated electrophiles,[23] and PFAS.[24–26] The dissociation and reductive cleavage of a given molecule were investigated based on the optimized electronic structures, bond dissociation energies and reduction potentials of the corresponding bond. The k_{exp} values represent the overall reactivities, and thus, the elementary reaction mechanisms of the overall reaction cannot be known. Calculating the one-electron reduction potential ($E^\circ_{red,aq}$, V) in the aqueous phase of each component in a given molecule can provide quantitative information about all possible reactive sites and help determine the rate-determining reaction mechanism with electrons, which is more advantageous than investigating conventional qualitative molecular descriptors such as lowest unoccupied molecular orbitals.

In this study, we use DFT to calculate the $E^\circ_{red,aq}$ values of conventional organic compounds with a wide variety of functional groups to determine the linear free energy relationships (LFERs) with the experimentally measured rate constants of e_{aq}^-. In addition, we use the 75 priority PFAS subset from the U.S. EPA[27] and calculate the $E^\circ_{red,aq}$ values of all possible elementary reactions of each PFAS to determine its dominant reaction mechanism and reactive sites. The determined LFERs of conventional organic compounds are used to predict the reactivities of e_{aq}^- with PFASs, which can be used as a screening tool for thousands of PFASs for electron-induced degradability. Fig. 1 demonstrates the flowchart of methods used in this study from the determination of LFERs for conventional organic compounds to the prediction of k_{chem} values for PFAS. While we demonstrate the prediction of k_{exp} values for e_{aq}^- in the homogeneous reduction processes, the reactivities of electrons *via* direct electron transfer on a heterogeneous-electrode can be extrapolated from the e_{aq}^- reactivities and the LFERs are also useful for the heterogeneous processes.

Materials and methods

According to the previous experimental studies reported in the literature, three major reaction mechanisms of e_{aq}^- include: (1) associative; (2) concerted dissociative; and, (3) stepwise dissociative mechanisms. In the associative mechanism, e_{aq}^- reacts with the π bond that can 'hold' an extra electron to form an anionic radical species.[20] Compounds containing carbonyl functional groups are examples of compounds that undergo associative reactions:

$$RC{=}O + e_{aq}^- \rightarrow R^{\bullet}CO^- \quad (1)$$

Both concerted and stepwise mechanisms involve bond cleavage. In the concerted mechanism, single-electron transfer to a parent compound and bond cleavage occur simultaneously, as shown in eqn (2). During the stepwise mechanism, the initial barrierless step of single-electron transfer results in the formation of an intermediate radical anion that has a longer lifetime than the bond vibration time (*i.e.*, 10^{-13} s).[28] The intermediate radical anion then undergoes bond cleavage, as shown in eqn (3). The nonexistence of a radical anion is a sufficient condition for the concerted mechanism to occur, but it is not a necessary condition. Thus, under the concerted mechanism, an intermediate radical anion may have a finite lifetime.[29]

$$RX + e_{aq}^- \rightarrow R^{\bullet} + X^- \quad (2)$$

$$RX + e_{aq}^- \rightarrow [RX]^{\bullet -} \rightarrow R^{\bullet} + X^- \quad (3)$$

In general, it is suggested that compounds containing a σ bond and/or a weak C–X bond are reduced *via* a concerted mechanism, and compounds containing a π bond (*e.g.*, C═S, S═S, NO_2, CN, C═C), strong C–X bonds (*e.g.*, C–F), and/or electron withdrawing groups (*e.g.*, –F, –CN, NO_2, –CO) are reduced *via* the stepwise mechanism.[23,30] However, caution should be taken for compounds with strong electron withdrawing groups and halogenated alkenes because a concerted mechanism could possibly occur due to an unstable intermediate radical anion or the requirement of reduced reaction barriers.[22,23]

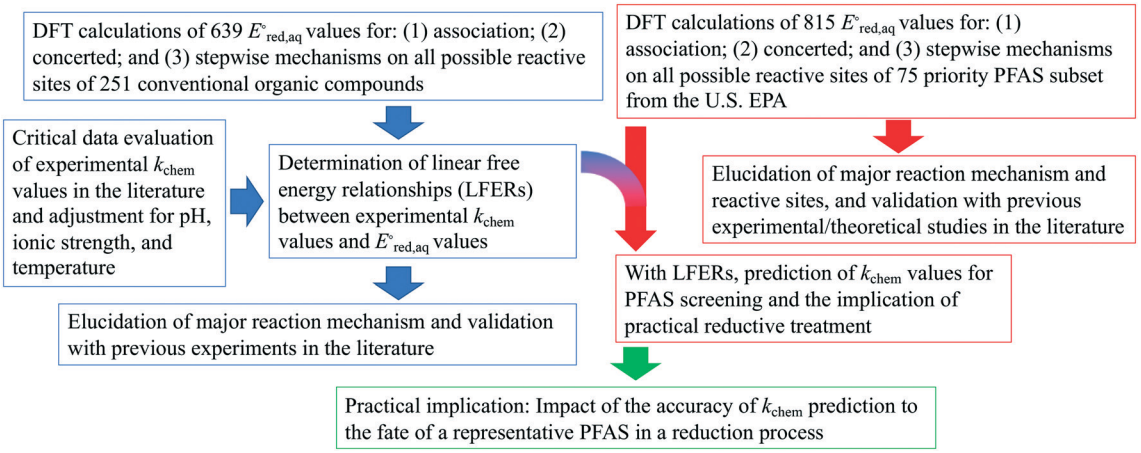

Fig. 1 Overall flowcharts of methodologies and logical steps.

To determine which of reduction mechanisms in eqn (1)–(3) is the rate-determining step for a given molecule, we explored the LFER that relates the experimentally measured chemical reaction rate constant, k_{chem}, and the $E^{\circ}_{red,aq}$ values relative to the standard hydrogen electrode (SHE) for each mechanism through the relation described by eqn (4). We, then, determined the dominant rate-determining reaction mechanism by investigating the correlation of each LFER. The concept of a LFER may be developed as below. Assuming an elementary reaction proceeds by the same reaction mechanism, the log of the rate constant and the log of the equilibrium constant are linearly related.[31] The natural log of the equilibrium constants has a linear relationship with the free energy reaction, ΔG^{react}_{aq}, which relates to the standard state reduction potential in eqn (5). Combining these two concepts enables the development of the LFER. Upon the calculation of the $\Delta E^{\circ}_{red,aq}$ values, all possible e_{aq}^- attacking sites for each compound were included, and the largest $E^{\circ}_{red,aq}$ value (*i.e.*, the smallest free energy of formation) in a given molecule was used for the determination of the LFER. We determined the LFER for each reaction mechanism listed in eqn (1)–(3) to investigate the correlation with k_{chem} values. The procedure to determine the k_{chem} values and the critical evaluation of literature-reported k_{exp} values are provided in Texts S1 in the ESI.†

$$\ln k_{chem} = -\alpha E^{\circ}_{red,aq} + \beta \quad (4)$$

In the above equation, α and β are the coefficients that determine the slope representing the relationship between the reductive ability of the reaction site and the observed overall kinetics and the intercept representing the kinetics at the reference electrode, respectively. We argue that the LFER is a useful way to relate the kinetics (*i.e.*, k_{chem} values) with thermodynamic parameters (*i.e.*, $E^{\circ}_{red,aq}$ values) and the LFER helps elucidate the dominant reaction mechanism. Determining the aqueous-phase free energies of activation, a parameter that drives the kinetics, for hundreds of reactions involving e_{aq}^- by investigating the potential energy surfaces (PES) of reactants and products is not practical for systematic investigation. Thus, we conducted PES scan to determine the reaction mechanism for a few compounds that may undergo more than one reaction mechanism described above.

For the associative and concerted reaction mechanisms, the $E^{\circ}_{red,aq}$ value was determined with eqn (5):

$$E^{\circ}_{red,aq} = -\left(\Delta G^{react}_{aq}/nF\right) - E^{\circ}(\mathrm{SHE}) \quad (5)$$

where n is the number of electrons transferred, F is Faraday's constant, and E°(SHE) = 4.28 V. Per the thermochemical (Born–Haber) cycle, ΔG^{react}_{aq}, may be expressed as:

$$\Delta G^{react}_{aq} = \Delta G^{react}_{gas} + \Delta\Delta G^{react}_{solv} \quad (6)$$

where ΔG^{react}_{gas} is the difference in the standard state gaseous phase Gibbs free energy of reaction between reactants and products and $\Delta\Delta G^{react}_{solv}$ is the difference in the standard state Gibbs free energy of solvation between reactants and products. All energies values were simulated at 298 K in this study.

Regarding the stepwise investigation, we calculated $E^{\circ}_{red,aq}$ with eqn (7),[26,32] which accounts for both the formation of the intermediate radical species and the resulting bond cleavage as an example of an RX bond.[26,32]

$$E^{\circ}_{red,aq} = \frac{1}{F} \times (-\mathrm{BDE} + T\Delta S - \Delta\Delta G_{solv}) + E^{\circ}_{X^{\cdot}/X^-} \quad (7)$$

where BDE is the bond dissociation energy of the cleaved bond, T is the absolute temperature in Kelvin, ΔS is the gaseous-phase entropy of the cleaved bond, $\Delta\Delta G_{solv}$ is the difference in solvation energy between the parent compound and the two radical products in eqn (8), and $E^{\circ}_{X^{\cdot}/X^-}$ is the reduction potential of the cleaved aqueous atom.

$$\Delta\Delta G_{solv} = \Delta G_{solv}(R^{\cdot}) + \Delta G_{solv}(X^{\cdot}) - \Delta G_{solv}(RX) \quad (8)$$

The BDE of the cleaved RX bond was calculated using the enthalpies (H) of the parent compound and the two radical products produced upon cleavage (eqn (9)).

$$BDE = -[H(RX) - H(R^{\bullet}) - H(X^{\bullet})] \quad (9)$$

To calculate the $E^{\circ}_{red,aq}$ values for the determination of LFERs, single point energy calculations at the M06-2X functional[33] and the Aug-cc-pVTZ basis set for all the mechanisms based on the optimized structures determined at M06-2X/cc-pVDZ or Aug-cc-pVTZ, unless detailed method was specified. We used M06-2X/LANL2DZ for compounds that contained iodine because the Dunning's basis set does not cover iodinated compounds. For PFASs, we used M06-2X with a combination of cc-pVDZ or Aug-cc-pVTZ basis set. Table S1 in the ESI† summarizes the method and basis set used for the group of compounds. M06-2X is specifically designed for the accurate treatment of long-distance interaction and/or the stronger electron-acceptor properties of the R$^{\bullet}$ fragments resulting from the dissociation of a C–R bond,[34] which makes it suitable for this study that investigates nucleophilic reactivity. The M06-2X functional was successfully applied for the reductive dissociation of polybrominated compounds.[23] A continuum form of the universal solvation model (SMD)[35] was used in the aqueous-phase calculations to account for the impact of an aqueous environment. It is noted that we did not aim to obtain the absolute $E^{\circ}_{red,aq}$ values of each elementary reaction, as they are computationally prohibitive when obtaining highly accurate ΔG^{react}_{aq} values for a number of compounds. Thus, we used M06-2X to obtain reliable relative $E^{\circ}_{red,aq}$ values so that we were able to relatively compare which reactive sites were dominant over other sites under the same reaction mechanism. The dominant reaction mechanism among the three major mechanisms was determined by the LFER with mechanistic insight into the reaction mechanisms, as the direct comparison of the $E^{\circ}_{red,aq}$ values obtained from eqn (5) and (7) was not possible. The validation of the M06-2X method with various basis sets is provided in Table S2 in the ESI.† All DFT calculations were performed using Gaussian16 (ref. 36) with the Michigan Tech high-performance cluster 'Superior' and homemade LINUX workstations.

Results and discussion

Determination of linear free energy relationships

Inconsistent experimental conditions (*e.g.*, pH, temperature, and ionic strength) were reported to measure k_{exp} values in a number of independent studies reported in the literature. Thus, the critical data evaluation of 268k_{exp} values (Text S1, Fig. S1 and Table S3 in the ESI†) in the literature selected 251k_{exp} values and calculated the chemical reaction rate constants by eliminating the diffusion contribution for the determination of LFERs (Text S1 in the ESI†). This critical data evaluation can potentially eliminate the uncertain k_{exp} values that may indicate significantly larger k_{exp} values that exceed the diffusion rate constant, k_D, in eqn (S1) in the ESI.† It should be noted that the diffusion rate constant, k_D, value used in eqn (S1)† has the limitations: (1) the Smoluchowski's equation to calculate the k_D values does not include either the long range forces between reactants or the diffusive displacement for small molecules; (2) the Smoluchowski's equation assumes the behavior of each reactant like a stationary sink around which a concentration gradient of the other reactant; and (3) the Smoluchowski's equation assumes the continuum structureless treatment of solvent.[31] Therefore, the extent of solvation effect may vary depending on the molecules. Thus, the k_D values we calculated may not represent the real diffusion rate constants. Nevertheless, the Smoluchowski's treatment has been successfully applied for many radical reactions (*e.g.*, hydroxyl radicals) and predicted the k_D in consistent with the experimental values.[38] As a consequence, we decided to adapt this approach in our calculations. Fig. 2 displays LFERs between the k_{chem} values and our theoretically calculated $E^{\circ}_{red,aq}$ values for 251 organic compounds undergoing three major mechanisms: (a) associative, (b) concerted, and/or (c) stepwise. Table 1 summarizes all the data used to determine the LFERs. Tables S4 and S5 in the ESI† contains all the $E^{\circ}_{red,aq}$ values for all possible reactive sites in a given molecule for the three reaction mechanisms. Regarding the association, we determined the LFER to be $\ln k_{chem} = 4.43E^{\circ}_{red,aq} + 31.76$ (r^2 = 0.72, N = 66, where N is the number of compounds for the development of the LFER) (Fig. 2a). When the carbon of the C═O functional group bonds with NH_2 or the OR functional group, the mesomeric effect of the –CO–NH_2– or –CO–OR– functional group occurs and decreases the double-bond character of the C═O functional group, creating new electrophilic centers with lower reactivity.[37] While we determined one unified LFER for associative mechanism with both C═O of ketones, aldehydes and carboxylate groups (blue dots in Fig. 1) and O of carboxylic acids, alcohols, esters, and amides (red dots in Fig. 1), the functional groups affect the associative mechanism with O in a different way from those with C═O functional group (see the next subsection). Compounds 17, 33, 45, and 153, whose k_{chem} values are close to or exceed the diffusion limit ($k_{chem} > 2.5 \times 10^{10}$ M^{-1} s^{-1}), were not included in either LFER. Compound 39, methyl trifluoroacetate, appear to be slightly off the LFER of the associative mechanism or that of the stepwise mechanism. Our investigation on the PES and spin density distribution supports the associative mechanism (see the detailed discussion in the reaction mechanism section below). Thus, we included this compound in the LFER of the associative mechanism. For the associative mechanism with the C═C of alkenes, the LFER was determined to be $\ln k_{chem} = 7.82E^{\circ}_{red,aq} + 41.25$ (r^2 = 0.63, N = 13) (Fig. 2b). The reactions of the alkenes with $k_{chem} > 5.3 \times 10^{9}$ M^{-1} s^{-1} were close to or exceeded the diffusion limit; therefore, the k_{chem} values did not change with an increase in the $E^{\circ}_{red,aq}$ values. The sample deviation (SD) calculated with eqn (10) was 0.084 for the associative mechanism and 0.13 for the associative mechanism with the C═C functional group. The SD values represent the

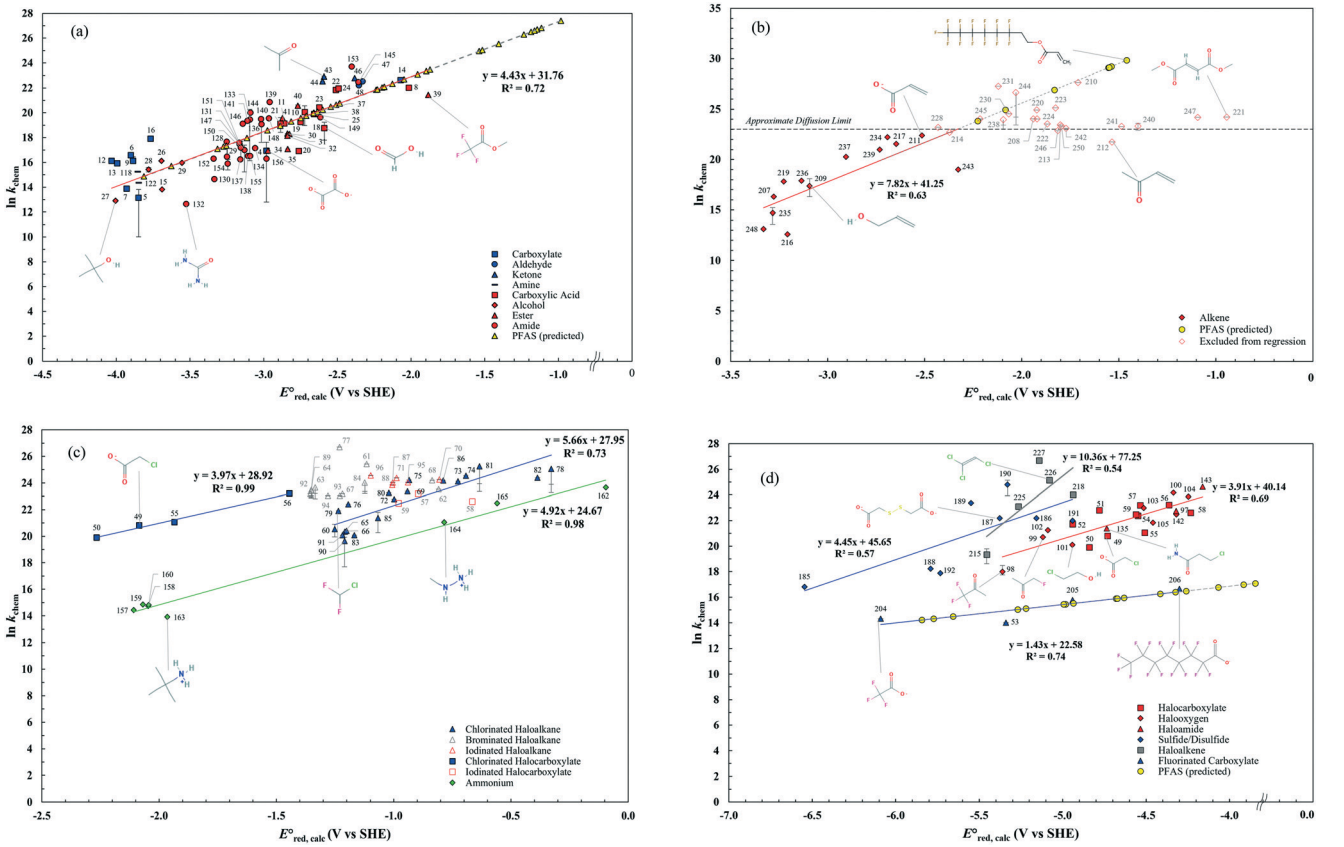

Fig. 2 LFERs for the (a) associative mechanism with C=O and O, (b) associative mechanism with C=C, (c) concerted mechanism, and (d) stepwise mechanism.

statistical distribution of the experimental k_{chem} values from the predicted values, $k_{predicted}$, within the normal distribution.[38]

$$SD = \sqrt{\frac{1}{n-1}\sum_{i=1}^{n}\left(\frac{k_{chem,i} - k_{predicted,i}}{k_{chem,i}}\right)^2} \quad (10)$$

For the concerted cleavage of the C–Cl bond of haloalkanes and halocarboxylate, we determined the LFERs to be $\ln k_{chem} = 5.66E^{\circ}_{red,aq} + 27.95$ ($r^2 = 0.73$, $N = 19$) and $\ln k_{chem} = 3.97E^{\circ}_{red,aq} + 28.92$ ($r^2 = 0.99$, $N = 4$), respectively (Fig. 2c). The SD values were 0.044 and 0.025, respectively. All the k_{chem} values of the haloalkane and halocarboxylate compounds that contain C–Br and C–I bonds were close to or exceeded the diffusion limit; therefore, we did not determine their LFERs. The presence of carboxylate functional groups impacted the $E^{\circ}_{red,aq}$ value of the cleavage of the C–Cl bond in the halocarboxylates; thus, a different LFER was determined for the group of chlorinated halocarboxylates. The four chlorinated carboxylates also appeared to adhere to the LFER for stepwise mechanism. According to experimental works, the group of these compounds undergo both concerted and stepwise mechanisms[21,22] and thus we keep these compounds in both LFERs. We also determined the LFER for the concerted cleavage of the C–N bond of alkyl ammonium (RNH_3^+) as $\ln k_{chem} = 4.92E^{\circ}_{red,aq} + 24.67$ ($r^2 = 0.98$, $N = 7$) (Fig. 2c) with the exception of tetramethylammonium (no. 166) and tetraethylammonium (no. 167), which contain a different base structure of $>N^+–C$. Additionally, we did not include compounds that contain oxygenated functional groups (no. 161, oxoethanaminium and no. 162, methoxyazanium) because of their dominant associative mechanism. The SD value was 0.051.

For the stepwise mechanism, we determined the LFERs for compounds with (1) haloalkanes that contain CO functional groups (*i.e.*, halocarboxylates, halooxygens and haloamides) or C–F bonds (fluorinated carboxylates), (2) haloalkenes, and (3) sulfides or disulfides for the stepwise mechanism to be the following: (1) $\ln k_{chem} = 3.96E^{\circ}_{red,aq} + 40.29$ ($r^2 = 0.69$, $N = 22$) or $\ln k_{chem} = 1.43E^{\circ}_{red,aq} + 22.58$ ($r^2 = 0.74$, $N = 4$), (2) $\ln k_{chem} = 10.36E^{\circ}_{red,aq} + 77.25$ ($r^2 = 0.54$, $N = 5$), and (3) $\ln k_{chem} = 4.45E^{\circ}_{red,aq} + 45.65$ ($r^2 = 0.57$, $N = 8$) (Fig. 2d). Because of the high strength of a C–F bond, the slope of the LFER for fluorinated carboxylates is significantly smaller than that of other haloalkanes. The SD values were 0.048 for haloalkanes, 0.26, for fluorinated carboxylates, 0.077 for haloalkenes, and 0.089 for disulfides. A detailed mechanistic discussion and prediction of PFAS are given below.

Table 1 $E^{\circ}_{red,aq}$ and k_{chem} values of 251 organic compounds used to determine the LFERs. Compounds in regular font are for associative mechanism, those in bold are for **concerted mechanism**, and those in italic are for *stepwise mechanism*

Class	No.	Name	Chemical formula	$\Delta G^{\circ}_{red,aq}$ (k_{cal} mol^{-1})	E°_{red} (V *vs.* SHE)	k_{chem} (M^{-1} s^{-1})	Reference for k_{exp}
Alkane	1	Methane	CH_4	25.97	−5.41	1.00×10^{7}	39
	2	Propane	$CH_3CH_2CH_3$	23.74	−5.31	2.10×10^{6}	40
	3	Butane	C_4H_{10}	22.77	−5.27	2.40×10^{6}	40
Carboxylate	4	Oxalate	$^{-}OOCCOO^{-}$	−29.94	−2.98	2.28×10^{7}	41–44
	5	Formate	$HCOO^{-}$	−9.93	−3.85	5.04×10^{5}	41, 45
	6	Succinate	$^{-}OOC(CH_2)_2COO^{-}$	−8.72	−3.90	1.59×10^{7}	37, 46
	7	Acetate	CH_3COO^{-}	−8.07	−3.93	1.05×10^{6}	45, 47
	8	Hydrogen oxalate	$HOOCCOO^{-}$	−52.21	−2.02	3.65×10^{9}	40
	9	Malonate	$^{-}OOC–CH_2–COO^{-}$	−9.07	−3.89	1.00×10^{7}	46
	10	Malonate(1−)	$HOOC–CH_2–COO^{-}$	−35.93	−2.72	5.06×10^{8}	46, 48
	11	Succinate(1−)	$HOOC(CH_2)_2COO^{-}$	−17.65	−3.51	2.05×10^{8}	37, 46
	12	Lactate	$CH_3CHOHCOO^{-}$	−5.70	−4.03	1.00×10^{7}	39
	13	Glycolate	$HOCH_2COO^{-}$	−6.61	−3.99	8.20×10^{6}	49
	14	Pyruvate	CH_3COCOO^{-}	−50.94	−2.07	6.80×10^{9}	39
	15	CID_4134252	$HOCH_2(CHOH)_4COO^{-}$	−13.59	−3.69	1.00×10^{6}	50
	16	Malate	$^{-}OOCCH_2CHOHCOO^{-}$	−11.81	−3.77	6.01×10^{7}	51
Carboxylic acid	17	Oxalic acid	$HOOCCOOH$	−62.94	−1.55	2.50×10^{10}	52
	18	Formic acid	$HCOOH$	−39.00	−2.59	1.41×10^{8}	45
	19	Succinic acid	$HOOC(CH_2)_2COOH$	−35.30	−2.75	2.30×10^{8}	46, 53
	20	Propionic acid	CH_3CH_2COOH	−35.03	−2.76	2.20×10^{7}	53
	21	Acetic acid	CH_3COOH	−32.16	−2.89	2.02×10^{8}	45, 54
	22	Malonic acid	$HOOC–CH_2–COOH$	−40.83	−2.51	3.03×10^{9}	46, 48, 53
	23	Lactic acid	$CH_3CH(OH)COOH$	−38.23	−2.62	7.36×10^{8}	46, 53
	24	Malic acid	$HOOCCH_2CH(OH)COOH$	−41.24	−2.49	3.41×10^{9}	55
	25	Glycolic acid	$HOCH_2COOH$	−37.42	−2.66	4.38×10^{8}	53
Alcohol	26	Methanediol	$CH_2(OH)_2$	−13.52	−3.69	1.00×10^{7}	45, 56
	27	*tert*-Butanol	$(CH_3)_3–C–OH$	−6.33	−4.01	4.00×10^{5}	47
	28	Butane-1,2,3,4	$HOCH_2[CH(OH)]_2CH_2OH$	−11.50	−3.78	5.00×10^{6}	57
	29	Mannitol	$HOCH_2[CH(OH)]_4CH_2OH$	−16.74	−3.55	8.50×10^{6}	57, 58
Ester	30	Methyl acetate	CH_3COOCH_3	−33.56	−2.82	8.73×10^{7}	59
	31	Methyl propionate	$C_2H_5COOCH_3$	−33.24	−2.84	9.03×10^{7}	37
	32	Ethyl propionate	$C_2H_5COOC_2H_5$	−33.22	−2.84	7.52×10^{7}	60
	33	Dimethyl oxalate	$CH_3OOCCOOCH_3$	−59.03	−1.72	1.04×10^{11}	48
	34	*tert*-Butyl acetate	$(CH_3)_3CCOOCH_3$	−30.20	−2.97	2.30×10^{7}	37
	35	2-Hydroxyethyl acetate	$CH_3COOCH_2CH_2OH$	−33.27	−2.84	2.60×10^{7}	61
	36	**Di-*tert*-butyl peroxide**	$\mathbf{(CH_3)_3–COOC(CH_3)_3}$	**44.93**	**−6.23**	$\mathbf{1.41 \times 10^{8}}$	62
	37	Methylene glycol monoacetate	$HOCH_2COOCH_3$	−37.37	−2.66	4.90×10^{8}	37
	38	Methyl methoxyacetate	$CH_3OCH_2COOCH_3$	−38.04	−2.63	4.48×10^{8}	63
	39	Methyl trifluoroacetate	CF_3COOCH_3	−42.28	−2.45	2.06×10^{9}	37
	40	Ethyl glycinate	$NH_2CH_2COOC_2H_5$	−34.86	−2.77	8.58×10^{8}	64
	41	Acetoxymethylamine	$H_2NCH_2COOCH_3$	−32.45	−2.87	3.14×10^{8}	37, 65
Ether	**42**	**Diethyl ether**	$\mathbf{(C_2H_5)_2O}$	**−38.95**	**−2.59**	$\mathbf{1.00 \times 10^{7}}$	20
Ketone	43	Acetone	CH_3COCH_3	−38.95	−2.59	8.90×10^{9}	66–70
	44	Methyl ethyl ketone	$CH_3CH_2COCH_3$	−38.72	−2.60	6.11×10^{9}	71
	45	2,3-Butanedione	$CH_3COCOCH_3$	−69.05	−1.29	1.67×10^{10}	48, 72
	46	Acetoin	$CH_3COCH(OH)CH_3$	−43.76	−2.38	7.95×10^{9}	72
Aldehyde	47	Acetaldehyde	CH_3CHO	−44.97	−2.33	6.11×10^{9}	45, 48
	48	Propionaldehyde	CH_3CH_2CHO	−44.42	−2.35	4.43×10^{9}	68, 71
Halocarboxylate	*49*	*Chloroacetate*	$ClCH_2COO^{-}$	*10.40*	*−4.73*	1.09×10^{9}	67, 69, 73–74
	50	*3-Chloropropanoate*	$Cl(CH_2)_2COO^{-}$	*12.92*	*−4.84*	4.40×10^{8}	73
	51	*Bromoacetate*	$BrCH_2COO^{-}$	*11.54*	*−4.78*	8.03×10^{9}	69
	52	*3-Bromopropanoate*	$Br(CH_2)_2COO^{-}$	*15.24*	*−4.94*	2.70×10^{9}	69
	53	*Fluoroacetate*	FCH_2COO^{-}	*66.82*	*−7.18*	1.20×10^{6}	69
	54	*2-Bromopropanoate*	$CH_3CHBrCOO^{-}$	*6.18*	*−4.55*	5.30×10^{9}	69
	55	*2-Chloropropanoate*	$CH_3CHClCOO^{-}$	*5.26*	*−4.51*	1.40×10^{9}	69
	56	*Trichloroacetate*	Cl_3CCOO^{-}	*1.91*	*−4.36*	1.22×10^{10}	69
	57	*2-Iodoacetate*	ICH_2COO^{-}	*5.89*	*−4.54*	1.20×10^{10}	69
	58	*2-Iodopropanoate*	$CH_3CHICOO^{-}$	*−1.08*	*−4.23*	6.60×10^{9}	69
	59	*3-Iodanylpropanoate*	$ICH_2CH_2COO^{-}$	*6.46*	*−4.56*	5.80×10^{9}	75
Haloalkane	**60**	**Chloromethane**	$\mathbf{CH_3Cl}$	**−69.84**	**−1.25**	$\mathbf{8.33 \times 10^{8}}$	**76–78**
	61	**Dibromomethane**	$\mathbf{CH_2Br_2}$	**−73.00**	**−1.11**	$\mathbf{1.10 \times 10^{11}}$	**79**
	62	**Bromoform**	$\mathbf{CHBr_3}$	**−80.06**	**−0.81**	$\mathbf{1.67 \times 10^{10}}$	**80**
	63	**Bromoethane**	$\mathbf{CH_3CH_2Br}$	**−67.93**	**−1.33**	$\mathbf{1.89 \times 10^{10}}$	**80–82**

Table 1 *(continued)*

Class	No.	Name	Chemical formula	$\Delta G^{\circ}_{red,aq}$ (k_{cal} mol^{-1})	E°_{red} (V *vs.* SHE)	k_{chem} (M^{-1} s^{-1})	Reference for k_{exp}
	64	**Bromopropane**	**$CH_3CH_2CH_2Br$**	**−67.55**	**−1.35**	**1.47×10^{10}**	**80, 82**
	65	**Chloropropane**	**$CH_3CH_2CH_2Cl$**	**−70.86**	**−1.21**	**6.85×10^{8}**	**40, 81, 82**
	66	**Chloroethane**	**CH_3CH_2Cl**	**−71.03**	**−1.20**	**7.21×10^{8}**	**77**
	67	**1-Bromo-2-chloroethane**	**CH_2ClCH_2Br**	**−70.61**	**−1.22**	**1.18×10^{10}**	**80**
	68	**Halothane**	**$CF_3CHClBr$**	**−79.44**	**−0.84**	**3.22×10^{10}**	**83**
	69	**1,1-Dichloroethane**	**CH_3CHCl_2**	**−77.00**	**−0.94**	**1.42×10^{10}**	**84**
	70	**Diiodomethane**	**CH_2I_2**	**−80.13**	**−0.81**	**3.40×10^{10}**	**79, 85**
	71	**Iodoethane**	**CH_3CH_2I**	**−75.94**	**−0.99**	**3.85×10^{10}**	**81, 82**
	72	**Dichloromethane**	**CH_2Cl_2**	**−75.69**	**−1.00**	**7.95×10^{9}**	**86**
	73	**Chloroform**	**$CHCl_3$**	**−81.97**	**−0.73**	**3.00×10^{10}**	**39**
	74	**Trichlorofluoromethane**	**CCl_3F**	**−82.75**	**−0.69**	**4.60×10^{10}**	**87**
	75	**Dichlorodifluoromethane**	**CF_2Cl_2**	**−77.16**	**−0.93**	**3.28×10^{10}**	**87**
	76	**Chlorotrifluoromethane**	**$CClF_3$**	**−71.19**	**−1.19**	**5.36×10^{9}**	**81**
	77	**Bromotrifluoromethane**	**CF_3Br**	**−70.32**	**−1.23**	**3.93×10^{11}**	**81**
	78	**Carbon tetrachloride**	**CCl_4**	**−91.15**	**−0.33**	**7.61×10^{10}**	**68, 88**
	79	**Chlorodifluoromethane**	**$CHClF_2$**	**−70.22**	**−1.24**	**3.29×10^{9}**	**89**
	80	**1,1,2-Trichloroethane**	**$ClCH_2CHCl_2$**	**−75.17**	**−1.02**	**1.27×10^{10}**	**84**
	81	**1,1,1-Trichloroethane**	**CH_3CCl_3**	**−84.09**	**−0.63**	**9.24×10^{10}**	**77, 84**
	82	**Hexachloroethane**	**CCl_3CCl_3**	**−89.80**	**−0.39**	**3.90×10^{10}**	**84**
	83	**2-Chlorobutane**	**$C_2H_5CH(Cl)CH_3$**	**−71.79**	**−1.17**	**5.21×10^{8}**	**82**
	84	**1,2-Dibromoethane**	**$BrCH_2CH_2Br$**	**−72.81**	**−1.12**	**2.74×10^{10}**	**80, 84**
	85	**1,2-Dichloroethane**	**$ClCH_2CH_2Cl$**	**−74.11**	**−1.07**	**1.91×10^{9}**	**84, 90**
	86	**1,1,2-Trichloro-1,2,2-trifluoroethane**	**$ClCF_2CCl_2F$**	**−80.52**	**−0.79**	**3.17×10^{10}**	**84**
	87	**1-Iodopropane**	**C_3H_7I**	**−75.56**	**−1.00**	**2.73×10^{10}**	**82**
	88	**1-Iodobutane**	**$CH_3(CH_2)_3I$**	**−75.50**	**−1.01**	**2.29×10^{10}**	**82**
	89	**1-Bromobutane**	**$CH_3(CH_2)_3Br$**	**−67.54**	**−1.35**	**1.59×10^{10}**	**80–82**
	90	**1-Chlorobutane**	**$CH_3(CH_2)_3Cl$**	**−70.83**	**−1.21**	**3.42×10^{8}**	**40, 54, 81, 82**
	91	**1-Chloro-2-methylpropane**	**$(CH_3)_2CHCH_2Cl$**	**−70.62**	**−1.22**	**5.21×10^{8}**	**82**
	92	**1-Bromopentane**	**$CH_3(CH_2)_4Br$**	**−67.45**	**−1.36**	**1.17×10^{10}**	**80**
	93	**2-Bromo-2-methylpropane**	**$(CH_3)_3CBr$**	**−70.36**	**−1.23**	**1.02×10^{10}**	**80**
	94	**2-Bromobutane**	**$CH_3CH_2CH(Br)CH_3$**	**−69.18**	**−1.28**	**1.01×10^{10}**	**80**
	95	**Trifluoroiodomethane**	**CF_3I**	**−77.06**	**−0.94**	**2.77×10^{10}**	**81**
	96	**Iodomethane**	**CH_3I**	**−73.39**	**−1.10**	**4.64×10^{10}**	**81, 91**
Halooxygen	*97*	*Isoflurane*	*$CHF_2OCHClCF_3$*	*0.87*	*−4.32*	*5.80×10^{9}*	84
	98	*1,1,1-Trifluoroacetone*	*CF_3COCH_3*	*24.93*	*−5.36*	*6.62×10^{7}*	*37*
	99	*Fluoroacetone*	*CH_3COCH_2F*	*19.34*	*−5.12*	*9.77×10^{8}*	*37*
	100	*Methoxyflurane*	*$CH_3OCF_2CHCl_2$*	*1.31*	*−4.34*	*3.16×10^{10}*	*84*
	101	*2-Chloroethanol*	*$ClCH_2CH_2OH$*	*15.25*	*−4.94*	*5.34×10^{8}*	*92*
	102	*2-Bromoethanol*	*$BrCH_2CH_2OH$*	*18.64*	*−5.09*	*1.71×10^{9}*	*69*
	103	*Chloroacetic acid*	*$ClCH_2COOH$*	*5.40*	*−4.51*	*9.60×10^{9}*	*93*
	104	*Chloral hydrate*	*$CCl_3CH(OH)_2$*	*−0.79*	*−4.25*	*2.31×10^{10}*	*94*
	105	*Enflurane*	*CHF_2OCF_2CHClF*	*4.14*	*−4.46*	*3.03×10^{9}*	*84*
Cyanide	106	Acetonitrile	CH_3CN	−14.83	−3.64	3.74×10^{7}	54, 68, 95
	107	Succinonitrile	$NC(CH_2)_2CN$	−21.84	−3.33	1.83×10^{9}	96
	108	**Trichloroacetonitrile**	**CCl_3CN**	**−98.67**	**0.00**	**3.20×10^{10}**	**84**
	109	Cyanamide	H_2NCN	−21.23	−3.36	1.60×10^{9}	96
Amine	110	Methylamine	CH_3NH_2	19.28	−5.12	9.00×10^{5}	97
	111	Butylamine	$CH_3(CH_2)_3NH_2$	17.07	−5.02	1.10×10^{6}	98
	112	Propylamine	$CH_3CH_2CH_2NH_2$	19.79	−5.14	1.10×10^{6}	98
	113	Ethylamine	$CH_3CH_2NH_2$	20.42	−5.17	1.00×10^{6}	98
	114	Isobutylamine	$(CH_3)_2CHCH_2NH_2$	18.63	−5.09	1.10×10^{7}	97
	115	Isoamylamine	$(CH_3)_2CHCH_2CH_2NH_2$	20.07	−5.15	1.00×10^{6}	97
	116	1,2-Dimethylhydrazine	$CH_3NHNHCH_3$	27.98	−5.49	6.10×10^{6}	99
	117	Methylhydrazine	CH_3NHNH_2	12.20	−4.81	6.50×10^{6}	99
	118	Glycinate	$NH_2CH_2COO^-$	−9.94	−3.85	1.70×10^{6}	100
	119	Ethanolamine	$H_2NCH_2CH_2OH$	−0.27	−4.27	2.00×10^{7}	101
	120	Isopropylamine	$(CH_3)_2CHNH_2$	18.20	−5.07	1.50×10^{6}	97
	121	*tert*-Butylamine	$(CH_3)_3CNH_2$	18.20	−5.07	1.10×10^{6}	97
	122	Beta-alaninate	$NH_2(CH_2)_2–COO^-$	−9.80	−3.85	4.20×10^{6}	102
	123	*N*,*N*-Diethylhydroxylamine	$(C_2H_5)_2NOH$	−2.51	−4.17	4.81×10^{7}	103
	124	*N*-Methyl-*N*-tritiohydroxylamine	CH_3NHOH	−15.92	−3.59	2.42×10^{8}	65
	125	Amylamine	$CH_3(CH_2)_4NH_2$	21.11	−5.20	1.00×10^{6}	98
	126	Trimethylhydrazine	$(CH_3)_2N–NHCH_3$	−16.76	−3.55	1.00×10^{8}	99
	127	1,1-Dimethylhydrazine	$(CH_3)_2NNH_2$	18.28	−5.07	2.40×10^{7}	99
Amide	128	Propionamide	$CH_3CH_2CONH_2$	−23.71	−3.25	4.66×10^{7}	100, 104

Table 1 *(continued)*

Class	No.	Name	Chemical formula	$\Delta G^{\circ}_{red,aq}$ (k_{cal} mol^{-1})	E°_{red} (V *vs.* SHE)	k_{chem} (M^{-1} s^{-1})	Reference for k_{exp}
	129	*N*-Ethylacetamide	$CH_3CONHC_2H_5$	−23.75	−3.25	1.40×10^7	64
	130	*N*-Methylacetamide	$CH_3CONHCH_3$	−21.79	−3.34	2.30×10^6	105
	131	Acetamide	CH_3CONH_2	−25.72	−3.16	3.84×10^7	74, 100, 106
	132	Urea	H_2NCONH_2	−17.40	−3.53	3.10×10^5	37, 74
	133	Glycinamide	$H_2NCH_2CONH_2$	−27.34	−3.09	2.83×10^8	65
	134	Formamide	$HCONH_2$	−28.17	−3.06	2.80×10^7	73, 100, 106, 107, 108
	135	*3-Chloropropionamide*	*$ClCH_2CH_2CONH_2$*	*10.52*	*−4.74*	*1.94×10^9*	*104*
	136	(*S*)-2-Hydroxypropanamide	$CH_3CH(OH)CONH_2$	−29.16	−3.02	1.91×10^8	49
	137	Aceturate	$CH_3CONHCH_2COO^-$	−25.84	−3.16	1.13×10^7	65, 109
	138	Pivalamide	$(CH_3)_3CCONH_2$	−27.03	−3.11	1.50×10^7	100
	139	Malonamide	$H_2NCOCH_2CONH_2$	−30.47	−2.96	1.15×10^9	110
	140	2-Hydroxyacetamide	$HOCH_2CONH_2$	−29.10	−3.02	2.93×10^8	49
	141	Biuret	$H_2NCONHCONH_2$	−26.98	−3.11	2.53×10^8	110
	142	*2-Chloropropionamide*	*$CH_3CH(Cl)CONH_2$*	*0.91*	*−4.32*	*7.58×10^9*	*104*
	143	*Iodoacetamide*	*ICH_2CONH_2*	*−2.75*	*−4.16*	*5.00×10^{10}*	*111*
	144	Hydroxyurea	$HONHCONH_2$	−27.45	−3.09	4.90×10^8	112
	145	Oxamate	$H_2NCOCOO^-$	−44.35	−2.36	5.70×10^9	110
	146	Succinamide	$H_2NCOCH_2CH_2CONH_2$	−26.23	−3.14	2.02×10^8	110
	147	Asparaginate	$H_2NCOCH_2CH(NH_2)COO^-$	−26.51	−3.13	2.40×10^7	113
	148	*N*,*N*-Dimethylformamide	$HCON(CH_3)_2$	−30.35	−2.96	3.08×10^8	100, 107, 108
	149	Methyl 2-acetamidoacetate	$CH_3CONHCH_2COOCH_3$	−38.38	−2.62	3.34×10^8	110
	150	2-Formamidoacetate	$HCONHCH_2COO^-$	−25.93	−3.16	2.90×10^7	110
	151	*N*-Methylformamide	$HCONHCH_3$	−25.68	−3.17	4.31×10^7	100, 108
	152	*N*-*tert*-Butylacetamide	$CH_3CONHC(CH_3)_3$	−21.69	−3.34	1.20×10^7	100
	153	Diacetamide	$(CH_3CO)_2NH$	−43.29	−2.40	1.98×10^{10}	110
	154	*N*,*N*-Diethylacetamide	$CH_3CON(C_2H_5)_2$	−23.89	−3.24	8.00×10^6	100
	155	*N*,*N*-Dimethylacetamide	$CH_3CON(CH_3)_2$	−27.42	−3.09	1.50×10^7	100, 105
	156		$(CH_3)_3CCON(CH_3)_2$	−29.95	−2.98	1.20×10^7	100
Ammonia	**157**	**Methyl ammonium hydride**	**$CH_3NH_3^+$**	**−50.08**	**−2.11**	**1.85×10^6**	**97, 113**
	158	**Ethylammonium**	**$C_2H_5NH_3^+$**	**−51.52**	**−2.05**	**2.50×10^6**	**98**
	159	**Trideuterio(propyl)azanium**	those in bold	**−50.99**	**−2.07**	**2.80×10^6**	**98**
	160	**Pentylazanium**	**$CH_3(CH_2)_4NH_3^+$**	**−51.57**	**−2.04**	**2.70×10^6**	**98**
	161	**2-Methoxy-2-oxoethanaminium**	**$H_3COOCCH_2NH_3^+$**	**−59.49**	**−1.70**	**6.80×10^9**	**65**
	162	**Methoxyazanium**	**$CH_3ONH_3^+$**	**−96.51**	**−0.10**	**1.90×10^{10}**	**65**
	163	***tert*-Butylammonium**	**$(CH_3)_3CNH_3^+$**	**−53.40**	**−1.96**	**1.10×10^6**	**97**
	164	**2-Methylhydrazinium**	**$CH_3NHNH_3^+$**	**−80.62**	**−0.78**	**1.40×10^9**	**99**
	165	**1,1-Dimethylhydrazinium**	**$(CH_3)_2NNH_3^+$**	**−85.83**	**−0.56**	**5.80×10^9**	**99**
	166	**Tetramethylammonium**	**$(CH_3)_4N^+$**	**−49.22**	**−2.15**	**5.60×10^6**	**114**
	167	**Tetraethylammonium**	**$(C_2H_5)_4N^+$**	**−52.94**	**−1.98**	**1.20×10^7**	**114**
Hydrogen sulfide	**168**	**Cysteaminium**	**$HSCH_2CH_2NH_3^+$**	**−51.15**	**−2.06**	**2.25×10^{10}**	**115, 116**
	169	**3-Sulfanylpropylazanium**	**$HS(CH_2)_3NH_3^+$**	**−52.08**	**−2.02**	**1.70×10^{10}**	**117**
Alkyne	170	Acetylene	HC triplet bond CH	−21.82	−3.33	2.00×10^7	118
	171	Propargyl alcohol	HC triplet bond CCH_2OH	−24.16	−3.23	2.12×10^8	68
Sulfate	172	Ethanesulfonate	$C_2H_5SO_3^-$	7.65	−4.61	3.50×10^7	119
Sulfoxide	*173*	*Dibutyl sulphoxide*	*$[CH_3(CH_2)_3SO(CH_2)_3CH_3]$*	*22.09*	*−5.24*	*3.60×10^6*	*120*
	174	*Di-tert-butyl sulfoxide*	*$[(CH_3)_3C]_2SO$*	*−63.62*	*−1.52*	*1.50×10^7*	*120*
	175	*Methyl (methylsulfinyl)methyl sulfide*	*$CH_3SOCH_2SCH_3$*	*22.05*	*−5.24*	*1.31×10^8*	*121*
Thiol	**176**	**Methanethiol**	**CH_3SH**	**−47.75**	**−2.21**	**1.08×10^{10}**	**122**
	177	**Thiolactate**	**$CH_3(CH)SHCOO^-$**	**−58.46**	**−1.75**	**2.89×10^9**	**116**
	178	**2-Mercaptopropionic acid**	**$CH_3CH(SH)COOH$**	**−62.50**	**−1.57**	**4.08×10^9**	**123**
	179	**Methyl thioglycolate**	**$HSCH_2COOCH_3$**	**−56.08**	**−1.85**	**1.12×10^{10}**	**116**
	180	**Beta-mercaptoethanol**	**$HS(CH_2)_2OH$**	**−49.88**	**−2.12**	**1.73×10^{10}**	**115, 124**
	181	**2-Methyl-2-propanethiol**	**$(CH_3)_3CSH$**	**−54.27**	**−1.93**	**3.41×10^9**	**122**
	182	**3-Mercaptopropionic acid**	**$HS(CH_2)_2COOH$**	**−50.10**	**−2.11**	**6.91×10^9**	**123**
	183	**Thioglycolate**	**$HSCH_2COO^-$**	**−54.30**	**−1.93**	**3.03×10^9**	**116**
	184		**$H_2NC(=NH)NHCH_2CH_2SH$**	**−51.25**	**−2.06**	**1.02×10^{11}**	**113**
Sulfide/disulfide	*185*	*Dimethylsulfide*	*CH_3SCH_3*	*52.27*	*−6.55*	*2.00×10^7*	*125*
	186	*3,3′-Dithiodipropionate*	*$(SCH_2CH_2COO^-)_2$*	*20.22*	*−5.16*	*4.35×10^9*	*126*
	187	*2,2′-Disulfanediyldiacetate*	*$(SCH_2COO^-)_2$*	*25.32*	*−5.38*	*4.30×10^9*	*126*
	188	*2,2′-Sulfanediyldiacetate*	*$S(CH_2COO^-)_2$*	*34.86*	*−5.79*	*8.30×10^7*	*116*
	189	*N-Acetylcysteamine*	*$CH_3CONHCH_2CH_2SH$*	*29.28*	*−5.55*	*1.43×10^{10}*	*116*
	190	*Cystamine*	*$S_2(CH_2CH_2NH_2)_2$*	*24.23*	*−5.33*	*5.85×10^{10}*	*126*
	191	*L-Cystine anion*	*$S_2[CH_2CH(NH_2)COO^-]_2$*	*15.24*	*−4.94*	*3.53×10^9*	*39, 115, 126, 127*

Table 1 *(continued)*

Class	No.	Name	Chemical formula	$\Delta G^{\circ}_{red,aq}$ (k_{cal} mol^{-1})	E°_{red} (V *vs.* SHE)	k_{chem} (M^{-1} s^{-1})	Reference for k_{exp}
	192	*3,3′-Thiodipropanoate*	*$S(CH_2CH_2COO^-)_2$*	*33.51*	*−5.73*	*5.80×10^7*	*116*
S^-	**193**	**2-Hydroxyethanethiolate**	**$HOCH_2CH_2S^-$**	**−15.20**	**−3.62**	**1.80×10^7**	**115**
	194	**2-Lambda1-sulfanylethanamine**	**$H_2NCH_2CH_2S^-$**	**−16.84**	**−3.55**	**9.55×10^8**	**115, 116**
	195	**2-Acetamidoethanethiolate**	**$CH_3CONHCH_2CH_2S^-$**	**−16.11**	**−3.58**	**1.90×10^9**	**116**
CS	196	Carbon disulfide	CS_2	−57.80	−1.77	3.10×10^{10}	128, 45
	197	Thiourea	H_2NCSNH_2	−18.12	−3.49	3.29×10^9	20
	198	Thiosemicarbazide	$H_2NNHCSNH_2$	−19.10	−3.45	1.15×10^9	129
	199	*N*,*N*′-Diethylthiourea	$CH_3CH_2NHCSNHCH_2CH_3$	−19.13	−3.45	5.10×10^8	129
Nitro	200	Nitromethane	CH_3NO_2	−61.02	−1.63	1.80×10^{11}	130–131
	201	1-Nitropropane	$CH_3CH_2CH_2NO_2$	−60.85	−1.64	2.70×10^{10}	132
	202	Nitroethane	$CH_3CH_2NO_2$	−60.17	−1.67	2.70×10^{10}	132
	203	2-Methyl-2-nitrosopropane	$(CH_3)_3C(NO)$	−63.46	−1.53	8.26×10^9	133
PFAS	*204*	*Trifluoroacetate*	*CF_3COO^-*	*76.90*	*−7.61*	*1.65×10^6*	*69, 134*
	205	*Perfluorobutanoic acid*	*$C_3F_7COO^-$*	*57.88*	*−6.79*	*7.10×10^6*	*134*
	206	*Perfluorooctanoic acid*	*$C_7F_{15}COO^-$*	*42.92*	*−6.14*	*1.70×10^7*	*134*
Alkene	207	Allylamine	$H_2C{=}CHCH_2NH_2$	−23.13	−3.28	1.20×10^7	97
	208	Acrylonitrile	$H_2C{=}CHCN$	−53.94	−1.94	2.78×10^{10}	135
	209	Allyl alcohol	$H_2C{=}CHCH_2OH$	−27.37	−3.09	3.47×10^7	54, 68, 70
	210	Acrylic acid	$H_2C{=}CHCOOH$	−59.27	−1.71	1.03×10^{12}	136
	211	Acrylate	$CH_2{=}CHCOO^-$	−40.74	−2.51	5.30×10^9	136
	212	Methyl vinyl ketone	$H_2C{=}CHCOCH_3$	−63.32	−1.53	2.78×10^9	137
	213	Methyl acrylate	$H_2C{=}CHCOOCH_3$	−57.17	−1.80	1.52×10^{10}	138
	214	Senecioic acid amide	$(CH_3)_2C{=}CHCONH_2$	−44.00	−2.37	7.23×10^9	139
	215	*Vinyl chloride*	*$CH_2{=}CHCl$*	*27.10*	*−5.45*	*2.53×10^8*	*140*
	216	Ethylene	$H_2C{=}CH_2$	−24.75	−3.21	3.00×10^5	54
	217	Ethenesulfonate	$CH_2{=}CHSO_3^-$	−37.67	−2.65	2.30×10^9	141
	218	*Tetrachloroethylene*	*$Cl_2C{=}CCl_2$*	*15.17*	*−4.94*	*2.67×10^{10}*	*90, 140*
	219	Crotonyl alcohol	$CH_3CH{=}CHCH_2OH$	−24.31	−3.23	5.51×10^7	54
	220	Crotonic acid	$CH_3CH{=}CHCOOH$	−54.36	−1.92	6.62×10^{10}	136
	221	Dimethyl fumarate	$CH_3OOCCH{=}CHCOOCH_3$	−76.95	−0.94	3.30×10^{10}	110
	222	Divinyl sulfone	$(H_2C{=}CH)_2SO_2$	−55.62	−1.87	1.66×10^{10}	137
	223	Methacrylic acid	$H_2C{=}C(CH_3)COOH$	−56.59	−1.83	8.26×10^{10}	136
	224	Methyl methacrylate	$H_2C{=}C(CH_3)COOCH_3$	−54.41	−1.92	2.72×10^{10}	139
	225	*trans-1,2-Dichloroethylene*	*$ClCH{=}CHCl$*	*22.70*	*−5.26*	*1.08×10^{10}*	*140*
	226	*Trichloroethylene*	*$ClCH{=}CCl_2$*	*18.45*	*−5.08*	*8.28×10^{10}*	*140*
	227	*cis-1,2-Dichloroethylene*	*$H_2C{=}CCl_2$*	*19.86*	*−5.14*	*3.86×10^{11}*	*140*
	228	1,3-Butadiene	$H_2C{=}CHCH{=}CH_2$	−42.65	−2.43	1.19×10^{10}	20
	229	Acetaldehyde oxime	$CH_3CH{=}NOH$	−30.63	−2.95	7.22×10^7	37
	230	*N*,*N*-Dimethylacrylamide	$CH_2{=}CHCON(CH_3)_2$	−51.04	−2.07	4.51×10^{10}	139
	231	Methacrylamide	$H_2C{=}C(CH_3)CONH_2$	−49.80	−2.12	7.10×10^{11}	139
	232	Cyanoguanidine	$NCN{=}C(NH_2)_2$	−31.89	−2.90	1.96×10^{10}	142
	233	*Tetracyanoethylene*	*$(NC)_2C{=}C(CN)_2$*	*36.90*	*−5.88*	*3.74×10^{10}*	*20*
	234	Methacrylate	$CH_2{=}C(CH_3)COO^-$	−36.63	−2.69	4.50×10^9	136
	235	3-Buten-1-ol	$H_2C{=}CHCH_2CH_2OH$	−22.99	−3.28	2.45×10^6	54, 68
	236	3-Buten-2-ol	$H_2C{=}CHCH(OH)CH_3$	−26.41	−3.13	5.91×10^7	54
	237	3-Methylbut-2-enoate	$(CH_3)_2C{=}CHCO_2^-$	−31.71	−2.91	6.40×10^8	143
	238	3,3-Dimethylacrylic acid	$(CH_3)_2C{=}CHCOOH$	−50.40	−2.09	2.53×10^{10}	136, 143
	239	Isocrotonate	$CH_3CH{=}CHCOO^-$	−35.70	−2.73	1.30×10^9	136
	240	Hydrogen fumarate	$HOOCCH{=}CHCOO^-$	−66.40	−1.40	1.35×10^{10}	48, 110
	241	Monomethyl fumarate	$CH_3OOCCH{=}CHCOO^-$	−64.43	−1.49	1.30×10^{10}	110
	242	2-Hydroxyethyl acrylate	$CH_2{=}CHCOOCH_2CH_2OH$	−57.85	−1.77	1.08×10^{10}	144
	243	*trans*-Aconitate(3−)	$^-OOCCH{=}C(COO^-)CH_2COO^-$	−45.03	−2.33	1.80×10^8	51
	244	Acrylamide	$H_2C{=}CHCONH_2$	−51.89	−2.03	3.81×10^{11}	45, 106, 107, 139, 145, 146
	245	Crotonamide	$CH_3CH{=}CHCONH_2$	−47.62	−2.22	2.75×10^{10}	139
	246	4-(Ethylamino)-4-oxobut-2-enoate	$C_2H_5NHCOCH{=}CHCOO^-$	−56.87	−1.81	8.50×10^9	99
	247	*cis*-Dimethyl fumarate	$CH_3OOCCH{=}CHCOOCH_3$	−73.51	−1.09	3.20×10^{10}	110
	248	4-Penten-2-OL	$H_2C{=}CHCH_2CH(OH)CH_3$	−21.90	−3.33	5.00×10^5	68
	249	Guanidine	$H_2NC(=NH)NH_2$	−4.98	−4.06	2.02×10^8	113
	250	Ethyl acrylate	$H_2C{=}CHCOOC_2H_5$	−57.33	−1.79	1.34×10^{10}	138
	251	Acetone oxime	$(CH_3)_2C{=}NOH$	−25.74	−3.16	3.29×10^8	37, 106

Impact of functional groups

The functional group(s) in the neighboring position of an e_{aq}^- attacking site substantially impact the reactivities with e_{aq}^-. In general, electron donating groups such as alkyl and amine functional groups in the neighboring position(s) decrease the nucleophilic reactivity of e_{aq}^- by increasing the electron density of the reactive site. For example, the negatively charged oxygen of the COO^- functional group acts as an electron donor to the adjacent C═O bond due to its lone pair of electrons and hence reduces the reactivity of e_{aq}^- in association with C═O. In contrast, electron withdrawing functional groups such as ketones and carboxylic acids decrease the electron density of the reactive site and hence increase the reactivity of e_{aq}^-. Fig. 3 plots the total sum of the Taft constants,[147] σ*, of neighboring functional group(s) against our $E^{\circ}_{red,aq}$ values for all the reaction mechanisms investigated in this study. The Taft constants of functional group(s) located in the neighboring position(s) of an e_{aq}^- attacking site are additive.[148,149] When the Taft constant of a functional group was not available, we used the value of a structurally similar functional group. Fig. S6 in the ESI† provides all the Taft constant values we used. Overall, we confirm the excellent correlations of all three reaction mechanisms, indicating that our theoretically calculated $E^{\circ}_{red,aq}$ values represent the general electron donating/withdrawing properties of the functional groups of aliphatic compounds. As expected, all correlations exhibit positive slopes, which confirm that larger $E^{\circ}_{red,aq}$ values represent stronger electron-withdrawing functional groups (*i.e.*, larger Taft constants). As shown by the LFERs in Fig. 2, larger $E^{\circ}_{red,aq}$ values correlate with larger overall k_{chem} values because of the increase in the nucleophilic reactivities of e_{aq}^-. Different correlations with Taft constants developed for the associative mechanism with CO and O confirm the different influence of

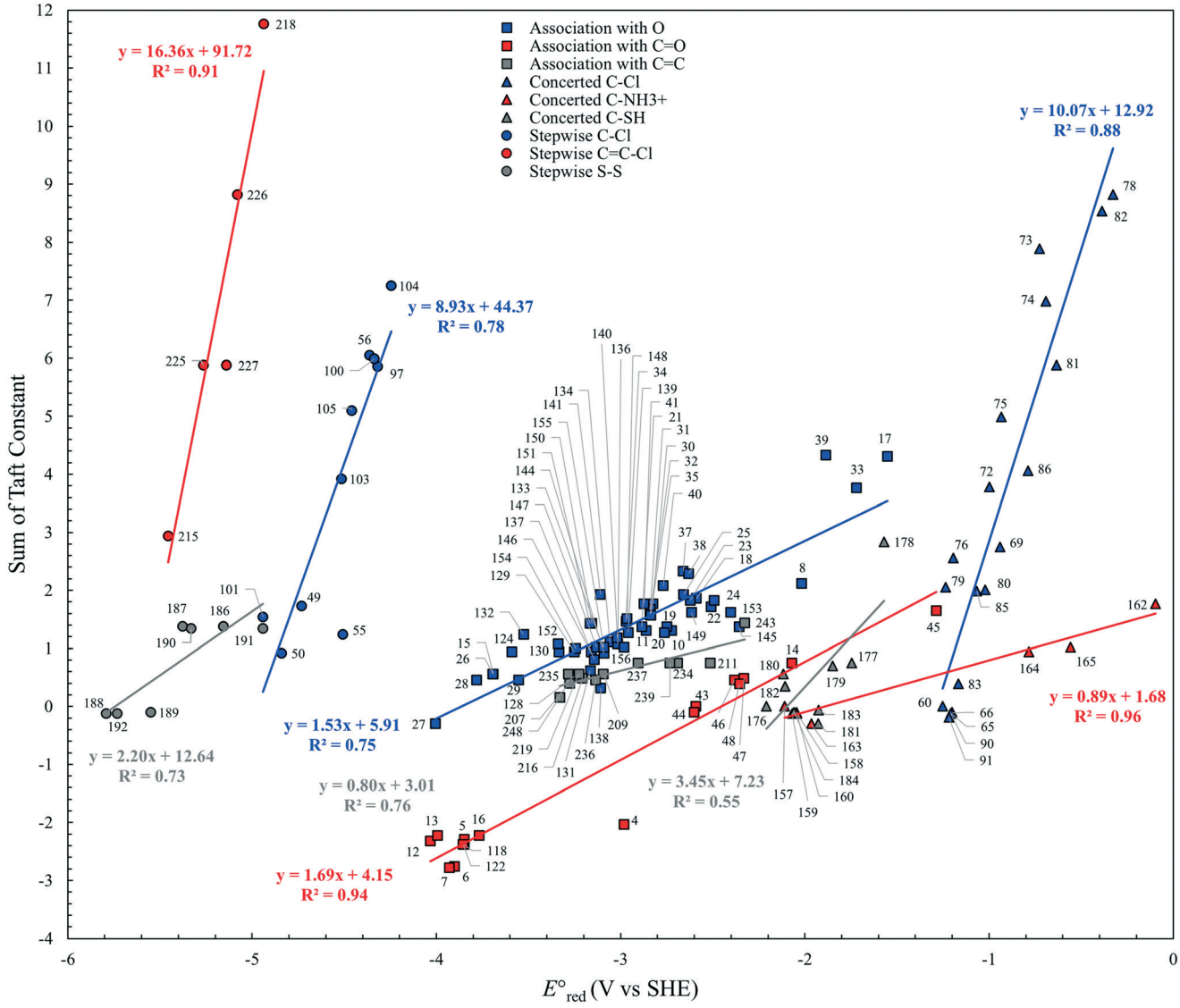

Fig. 3 Sum of Taft constants against the theoretically calculated $E^{\circ}_{red,aq}$ values of each compound.

neighboring functional groups resulting from inductive and mesomeric effects. The smaller slope (1.53) for the associative mechanism with O than that (1.69) for the associative mechanism with CO indicates the inhibition of reactivity resulting from the mesomeric effect. Hart *et al.*[37] examined the negative slope between $\log k_{exp}$ and the Taft constants for groups of ketones with a limited number of data (N = 10) and concluded that the slowing effect due to the mesomeric effect was more extensive than expected from inductive electron-donating/withdrawing effects. They also acknowledged that both mesomeric and inductive effects could apply to carboxylic compounds (N = 3), and their data appeared to adhere to both correlations well. Notably, two compounds that we propose for the stepwise cleavage mechanism of the C–F bond of CF_3COCH_3 (no. 98) and CH_3COCH_2F (no. 99) (see discussion on the reaction mechanism below) were included in the correlation with the Taft constant for the associative mechanism with CO by Hart. If these compounds and carboxylic compounds were removed from their correlation, a handful of compounds (N = 4) would remain in close proximity, and a negative correlation between the k_{chem} values and the sum of Taft constants would not be observed. Most likely, our extensive analysis of data (N = 66) and the use of $E^{\circ}_{red,aq}$ values revealed a better comprehensive picture of the impact of functional groups.

Neighboring functional groups also affect the concerted cleavage mechanism of each C–Cl, C–NH_3^+, and S–S bond as well as the stepwise cleavage mechanism of each C–Cl and S–S bond. The slopes of the correlations for C–Cl bond cleavage for both concerted and stepwise mechanisms were found to be significantly steeper than those for C–N and C–S cleavages. The similar slopes of the correlations for C–Cl bond between concerted and stepwise mechanisms indicate that the impact of neighboring functional groups is similar despite of the formation of intermediate species in the stepwise mechanism. While the Taft constants for C–C bond cleavage were substantially different for various functional groups in the neighboring positions, the range of $E^{\circ}_{red,aq}$ values was within approximately 1 V. These results indicated the higher sensitivity of the $E^{\circ}_{red,aq}$ values associated with the properties of the electron-donating/withdrawing functional groups when compared with those examined for C–N and S–S bonds.

Reaction mechanisms

Associative mechanism. When the π-fragment of a CO functional group is present in ketone, aldehyde and carboxylate, the initial injection of an electron occupies low-energy π*-orbitals *via* associative mechanism to form a carbon-centered radical.[150,151] However, it is unclear whether association with C═O is maintained or the stepwise cleavage of a C–X bond occurs in the group of halooxygens.[21,22,152] Our investigation of the PES of methyl trifluoroacetate (no. 39) and the product of radical anion as a function of one of dihedral angles showed the merging point of these PESs at approximately −70 degree (Fig. S2 in the ESI†), indicating the possibility of stepwise dissociative mechanism. However, the spin density distributions of elongated C–F bond structures were located on the acetate carbonyl functional group with an increase in one of the C–F bonds, which confirmed the associative mechanism (Fig. S3 in the ESI†). Our investigation on the lowest unoccupied molecular orbital (LUMO) represents no antibonding orbitals with regard to the C–F bond (Fig. S4 in the ESI†), supporting the initial electron association with the CO functional group.

The mesomeric effect described in the overall results move the reaction center from the C═O functional group of carboxylic, ester, and acetamide compounds to the alkoxyl group of O. The partial positive charge generated on OH of carboxylic and alcohol, C–O of ester, C–N of acetamide is the site of e_{aq}^- addition in the mesomeric form, which were confirmed by our analysis on the charge distribution (Fig. S5 in the ESI†). Although concerted cleavage of a C–O bond of esters or alcohol could occur, a better correlation of LFER for the association with O than those for the concerted cleavage of a C–O bond is the evidence for the dominant associative mechanism (Fig. S6 in the ESI†).

The k_{chem} values range from 10^7 to 10^{12} M^{-1} s^{-1} for the group of alkenes and some k_{exp} values are very close to or exceed the diffusion-limited rate. The association of e_{aq}^- with one of unsaturated carbons generates a radical anion intermediate described as a 3-electron 2-orbital state of π character[22] with carbon atoms that are sp3 hybridized with a dangling lone pair of electrons on one carbon atom and an unpaired radical electron on the other carbon atom. The initial injection of an electron produces a carbon-centered radical that further undergoes the reaction with second e_{aq}^- to produce a stable unsaturated carbon after leaving the halogen functional group.

The group of nitro compounds include three k_{chem} values for nitromethane (no. 200), 1-nitropropane (no. 201), and nitroethane (no. 202). The k_{chem} values for all the compounds are greater than 10^{10} M^{-1} s^{-1} exceeding the diffusion-limited. Our E°_{aq} values for the associative mechanism are approximately −1.6 V for all the compounds, whereas those for the concerted cleavage of C–NO_2 bond are approximately −2.2 V. This indicates the preference of the associative mechanism with e_{aq}^- and is supported by the spin density distribution on the NO_2 functional group (Fig. S7 in the ESI†). Due to the few datasets, we were not able to develop the LFER.

Concerted dissociative mechanism

Haloalkane and halocarboxylate. The concerted dissociative cleavage of a C–X (X = Cl, Br, and I) bond of haloalkanes is supported by the presence of σ* antibonding orbitals with respect to the C–X bond. Injection of an electron into such orbitals is accompanied by the barrierless dissociation of the C–X bond and the reductive cleavage follows the concerted dissociative mechanism.[21,22,153] Despite the fact that a carboxylate functional group was present in the given molecular structure of haloalkanes, we observed that the

weak C–X (X = Br and I) bond of halocarboxylates underwent concerted reduction due to the inability to hold the e_{aq}^-. We investigated the spin density distribution in a given molecule to identify a possible attacking site by e_{aq}^-. The spin density distribution on four chlorinated carboxylates indicates the solvated electron was located on the carbon atom in the C–Cl group (Fig. S8 in the ESI†), suggesting that the C–Cl bond cleavage could occur upon the attack by the e_{aq}^-. It should be noted that we observed the significant elongation of a C–Cl bond upon the structure optimization for 2-chloropropanoate (3.77 Å of C–Cl) and trichloroacetate (3.58 Å of C–Cl). This bond elongation suggests that the C–Cl bonds may not cleave upon the attack by the solvated electron, and thus the stepwise reduction mechanism may occur. The e_{aq}^- was likely held in the σ* antibonding orbital of chlorine, forming an intermediate radical anion species. Because of the uncertainty of the aqueous-phase PES, we were not able to confirm the dominant mechanism on these two chlorinated carboxylates. The detailed investigation on the PES for this group of compounds are underway.

The brominated and iodinated species appeared to undergo concerted reduction. In all radical anion structures, the C–X (X = Br or I) bond was elongated significantly and the e_{aq}^- was located on the carbon of the C–X group (Fig. S9 and S10 in the ESI†). Because we did not observe any associative mechanism of e_{aq}^- with the C═O functional group, the stepwise reduction mechanism seemed to be unlikely. The concerted mechanism is reasonable because the C–Br bond strength is also relatively weak (285 kJ mol^{-1}) compared to C–Cl and C–F, which is consistent with experimental finding.[23]

The C–N bond in general undergoes concerted dissociative cleavage. We determined two LFERs of ammonium compounds undergoing concerted and associative mechanisms and confirmed the concerted cleavage of a C–N bond of ammonium functional group for the rate determining step (Fig. S11 in the ESI†). The group of cyanide included 3k_{chem} values of acetonitrile (no. 106), succinonitrile (no. 107), and cyanamide (no. 109). While the k_{chem} value of acetonitrile was 10^7-th order, the other two were 10^9-th order. Our E_{aq}° values for the concerted cleavage of C–CN bond for these compounds ranged from −3.33 V to −3.06 V, whereas those for the association were from −3.64 V to −3.33 V. These indicate the preference of concerted cleavage of C–CN bond to form cyanide ion (CN^-) and carbon-centered radicals. Our investigation on the spin density of cyanide compounds indicated the high spin density at the cyanide functional group (Fig. S12 in the ESI†). Due to the small number of compounds, we were not able to develop the LFER.

The group of thiol contained 12 compounds containing at least one –SH functional group. As discussed above, the C–S bond is generally the weak point of a molecule because of its bond weakness in comparison to the C–C and C–H bonds. In the thiol compounds, the e_{aq}^- likely attacks the C–S group and results in the immediate bond cleavage due to a lack of antibonding σ* orbitals on the –SH functional group to hold the extra electron. Or the e_{aq}^- associates with the C═O bond and loosens the C–S bond to cleave in the stepwise mechanism. Among all compounds containing thiol functional group, we did not observe any clear LFERs for both mechanisms (Fig. S13 in the ESI†). However, for thiols that do not contain C═O functional group, we observed the acceptable LFER for concerted mechanism due to the limited number of data. Therefore, this class of compounds is likely reduced by the concerted mechanism, generating $R^{\bullet}$ and HS^-.[154]

Stepwise mechanism

Halocarboxylates, halooxygens, chlorinated amides and haloalkenes. We observed the consistent stepwise mechanisms for halocarboxylates (no. 49–59), halooxygens (no. 97–105), and chlorinated amides (no. 135 and no. 142) because of the presence of COO^-, OH and CO functional groups, which are consistent with previous experimental observations.[20–22] When haloalkanes contain electron-withdrawing and π-acceptor functional groups or other π-fragments, the electrons may initially occupy low-energy π*-orbitals and the reduction of these molecules may result in the transient formation of radical anions.[155] For the fluorinated carboxylates (no. 53 and 204–206), we determined the different trend from other halocarboxylates because of the abnormally strong C–F bond. While the optimized structure did not show the elongation of the C–F bond, our spin density observation of fluoroacetate confirms the association of e_{aq}^- with the carboxylate functional group (Fig. S14 in the ESI†). In addition, the lowest unoccupied molecular orbital (LUMO) of fluoroacetates confirms antibonding orbitals with regard to the C–F bonds (Fig. S15 in the ESI†). The singly occupied molecular orbitals (SOMO) of the vertically excited radical anions $(C\text{–}F^{\bullet-})^*$ are characterized by essentially the same shapes (Fig. S16 in the ESI†). Geometry optimization of these intermediate radical anion resulted in the significant elongation of one of the C–F bonds and formation of the $\{C\cdots F\}^{\bullet-}$. The electronic structure of the radical anion intermediate as a 3-electron 2-orbital state of p character with carbon atoms that are sp3 rather than sp2 hybridized with a dangling lone pair of electrons on one carbon atom and an unpaired radical electron on the other carbon atom.

Electron-withdrawing functional groups adjacent to a CO functional group induce a shortening of the C═O bond[156] (*e.g.*, 1.30 Å of CF_3COCH_3 (no. 98) and 1.31 Å of CH_3COCH_2F (no. 99) compared to 1.32 Å of CH_3COCH_3 from our optimized structures), which leads to a lower electron density in the π orbitals, resulting in the higher reactivity toward e_{aq}^-. However, the k_{chem} values of CF_3COCH_3 and CH_3COCH_2F do not appear to follow this trend and show substantially smaller rate constants (*i.e.*, 10^7–10^8 M^{-1} s^{-1}) for associative mechanism. We propose that these two compounds undergo stepwise mechanism where e_{aq}^- associates with CO π bond and elongates the C–F bond, followed by the cleavage of the C–F bond. The $E_{red,aq}^{\circ}$ values

of these compounds for the stepwise mechanism are −5.36 V for CF_3COCH_3 and −5.12 V for CH_3COCH_2F. We confirmed that these $E^{\circ}_{red,aq}$ values adhere to the LFER developed for halooxygen/halocarboxylate undergoing stepwise. It should be noted that the aqueous-phase PES of radical anions of these compounds (*i.e.*, intermediate) as a function of dihedral angle has uncertainties in the energy values and we were not able to confirm the stepwise mechanism. Our investigation on the spin density distribution shown in Fig. S17–S20† for both compounds provide the evidence of electron association and elongation of the C–F bond, which support the stepwise mechanism. Furthermore, the LUMO of both compounds (Fig. S21†) was the evidence of stepwise cleavage that holds the electron in one of the C–F bonds. Based on our investigation, we only propose stepwise mechanisms for these two compounds and further study is needed to confirm the reaction mechanism.

Sulfides, disulfides, sulfoxide. A total of 8 compounds were investigated for the group of sulfides that contain a –C–S–C– functional group and disulfide that has a –C–S–S–C– functional group. We determined the LFER for the stepwise mechanism that cleave the C–S bond of sulfides and the S–S bond of disulfides. We did not observe any correlation for the concerted mechanism (Fig. S22a in the ESI†). Although some sulfides (no. 186, 187, 191, and 192) contain COO^- functional group that implicates the initial association with e_{aq}^-, those functional groups are located far from the C–S and S–S sites and do not appear to impact the elongation of those bonds upon the injection of a first electron. Upon the attack by e_{aq}^-, the S–S or C–S bond initially elongates which results in a decrease in the energy of the antibonding σ* orbital that localizes over the elongated S–S or C–S bond. This antibonding orbital temporarily holds the e_{aq}^- for more than one vibration, creating a three-electron bonded radical anion intermediate structure $CSSC^{\bullet-}$ or a C-centered radical.[157] After the formation of this radical anion, the S–S bond cleaves, resulting in the following products: $RS^{\bullet}$ and RS^- *via* a stepwise mechanism.[158,159]

The sulfoxide class (no. 173–175) has the characteristic of a central S═O double bond. The presence of a π-bond which allows for electron localization, accessible antibonding π* orbitals, and two weak C–S bonds suggest that this class of compounds is reduced *via* the stepwise mechanism. The e_{aq}^- likely attacks the sulfur atom, resulting in the elongation of a C–S bond, as was observed in the sulfide and disulfide class. Simultaneously, the π-bond transforms into a σ bond by shifting two electrons to the oxygen atom, creating a negative charge on the oxygen.

Alkanes and amines. Compounds belonging to alkane and amines are generally difficult to reduce due to a lack of electron withdrawing functional groups in their chemical structures. We estimated E°_{aq} values for the alkane class to be low with the values ranging from −5.27 V to −5.41 V. The k_{chem} values are also significantly small in the range from 10^6 and 10^7 M^{-1} s^{-1}. For these reasons, we do not include any data in the groups of alkanes and amines in the analysis of LFERs.

Prediction of the reactivities with per- and polyfluoroalkyl substances (PFASs)

We investigate the reactivities of e_{aq}^- with the 75 priority PFAS subset from the U.S. EPA. The 75 PFASs were grouped based on the functional groups. The $E^{\circ}_{red,aq}$ values for (1) the associative mechanism with C═O and influenced by $\pi^*_{C=O}$ orbitals,[160,161] (2) the associative mechanism with O, and (3) the stepwise C–F cleavage mechanism for all possible attacking sites in a given PFAS are summarized in Table 2. Fig. 4 displays the range of $E^{\circ}_{red,aq}$ values for the stepwise cleavage of a C–F bond at different positions for the selected groups of PFASs investigated in this study. For this plot, we used M06-2X/cc-pVDZ for both structural optimization and frequency calculations and used the LFER determined from the same method to avoid significant computational time. Notably, we verified that the trend of all energies from representative PFASs was consistent between M06-2X/cc-pVDZ and M06-2X/Aug-cc-pVTZ (Table S6 in the ESI†). The group of polyfluorocarboxylates (PFCAs) has 7 PFASs with $E^{\circ}_{red,aq}$ values in the range from −4.1 V to −2.3 V for the associative mechanism with C═O and in the range from −7.3 V to −6.0 V for the stepwise C–F cleavage mechanism. From the largest $E^{\circ}_{red,aq}$ value in each reaction mechanism along with the LFER ($\ln k_{chem} = 1.82E^{\circ}_{red,aq} + 27.80$ in Fig. S23 in the ESI†), the k_{chem} values in neutral solution were predicted to range from 6.9×10^7 M^{-1} s^{-1} to 3.8×10^{10} M^{-1} s^{-1} for the associative mechanism and 4.5×10^6 M^{-1} s^{-1} to 2.1×10^7 M^{-1} s^{-1} for the stepwise cleavage mechanism of a C–F bond. The predicted k_{chem} values of perfluorobutanoic acid (3 carbon chains, 6.87×10^7 M^{-1} s^{-1}), perfluorohexanoic acid (5 carbon chains, 6.66×10^8 M^{-1} s^{-1}), perfluorooctanoic acid (7 carbon chains, 5.78×10^8 M^{-1} s^{-1}) and perfluorononanoic acid (8 carbon chains, 7.96×10^8 M^{-1} s^{-1}) for the associative mechanism with C═O were in excellent agreement with the recently reported k_{exp} values of $(5.4 \pm 1.2) \times 10^8$ M^{-1} s^{-1} for perfluorobutanoic acid, $(5.4 \pm 0.1) \times 10^8$ M^{-1} s^{-1} for perfluorohexanoic acid, $(7.1 \pm 0.6) \times 10^8$ M^{-1} s^{-1} for perfluorooctanoic acid, and $(6.4 \pm 0.4) \times 10^8$ M^{-1} s^{-1} for perfluorononanoic acid.[162] Although this experimental study did not determine the mechanism for those measured rate constants, we believe they measured the rates of the associative mechanism. In contrast, the k_{exp} values for C–F cleavage (10^6–10^7 M^{-1} s^{-1}) were previously reported[134] and used for the determination of our LFERs (compound no. 204–206), which confirm the significantly smaller k_{chem} values of the stepwise cleavage mechanism of a C–F bond. The predicted k_{chem} values in three reaction mechanisms for all 75 PFASs are shown in Fig. S24 in the ESI.† The k_{chem} values that exceeded the diffusion limit (3×10^{10} M^{-1} s^{-1} and $\ln k = 24.1$) were not included in either figure. The k_{chem} values predicted for the 75 PFASs that undergo the stepwise cleavage mechanism of a C–F bond range from 6.9×10^7 to 3.7×10^8 M^{-1} s^{-1}. In contrast, $19k_{chem}$ values range from 4.9×10^7 M^{-1} s^{-1} to 3×10^{10} M^{-1} s^{-1} for the associative mechanism with C═O, $23k_{chem}$ values range from 1.3×10^6 to 3×10^{10} M^{-1} s^{-1} for the associative mechanism

Table 2 The $E^{\circ}_{red,aq}$ values calculated for all possible attacking sites in PFASs

Class	Compound name	Attacking site	2D structure	E°_{red} (V *vs.* SHE) Stepwise (C–F cleavage)	Concerted (C–F cleavage)	Association with functional group
PFCA	Perfluorobutanoic acid (PFBA)	Alpha	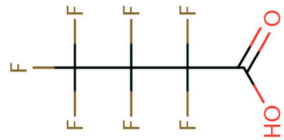	−6.86	−3.45	−4.10
		Beta		−7.13	−3.69	
		Terminal		−7.46	−4.05	
	Perfluorooctanoic acid (PFOA)	Alpha	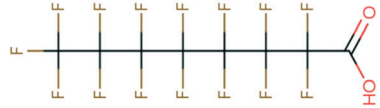	−6.14	−3.48	−3.50
		Beta		−6.28	−3.62	
		Gamma		−6.25	−3.58	
		Delta		−6.24	−3.56	
		Epsilon		−6.30	−3.55	
		Zeta		−6.30	−3.60	
		Terminal		−6.66	−4.01	
	Perfluorohexanoic acid	Alpha	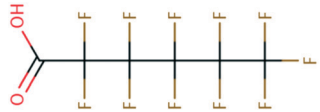	−6.49	−3.49	−3.46
		Beta		−6.60	−3.62	
		Gamma		−6.63	−3.56	
		Delta		−6.68	−3.62	
		Terminal		−7.02	−4.02	
	Perfluorononanoic acid	Alpha		−6.01	−3.53	−3.41
		Beta		−6.12	−3.65	
		Gamma		−6.10	−3.60	
		Delta		−6.09	−3.59	
		Epsilon		−6.12	−3.57	
		Zeta		−6.12	−3.52	
		Eta		−6.12	−3.60	
		Terminal		−6.55	−4.08	
	Ammonium perfluorooctanoate	Alpha	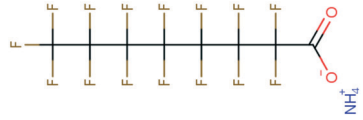	−6.14	−3.48	−3.50
		Beta		−6.28	−3.62	
		Gamma		−6.25	−3.58	
		Delta		−6.24	−3.56	
		Epsilon		−6.30	−3.55	
		Zeta		−6.30	−3.60	
		Terminal		−6.66	−4.01	
	Methyl heptafluorobutyrate	Alpha	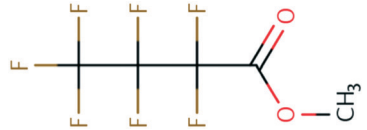	−6.52	−3.33	−2.32
		Beta		−6.89	−3.65	
		Terminal		−7.29	−4.07	
	Methyl perfluorohexanoate	Alpha	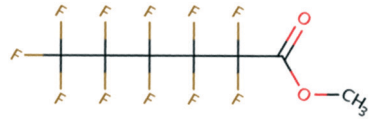	−6.20	−3.32	−2.43
		Beta		−6.53	−3.61	
		Gamma		−6.48	−3.54	
		Delta		−6.51	−3.57	
		Terminal		−6.87	−4.00	

Table 2 *(continued)*

Class	Compound name	Attacking site	2D structure	E°_{red} (V *vs.* SHE) Stepwise (C–F cleavage)	Concerted (C–F cleavage)	Association with functional group
PFSA	Perfluorobutanesulfonic acid	Alpha		−6.69	−3.56	−2.79
		Beta		−6.71	−3.56	
		Gamma		−6.60	−3.48	
		Terminal		−7.04	−3.93	
	Perfluorooctanesulfonic acid	Alpha		−6.08	−3.64	−3.31
		Beta		−5.94	−3.53	
		Gamma		−5.96	−3.53	
		Delta		−5.99	−3.53	
		Epsilon		−6.00	−3.54	
		Zeta		−6.05	−3.55	
		Eta		−6.02	−3.56	
		Terminal		−6.58	−4.40	
	Potassium perfluorooctanesulfonate	Alpha		−6.08	−3.64	−3.31
		Beta		−5.94	−3.53	
		Gamma		−5.96	−3.53	
		Delta		−5.99	−3.53	
		Epsilon		−6.00	−3.54	
		Zeta		−6.05	−3.55	
		Eta		−6.02	−3.56	
		Terminal		−6.58	−4.40	
	Potassium perfluorobutanesulfonate	Alpha	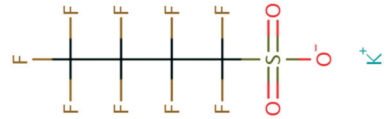	−6.69	−3.56	−2.79
		Beta		−6.71	−3.56	
		Gamma		−6.60	−3.48	
		Terminal		−7.04	−3.93	
	Potassium perfluorohexanesulfonate	Alpha		−6.45	−3.65	−3.43
		Beta		−6.25	−3.50	
		Gamma		−6.34	−3.55	
		Delta		−6.40	−3.55	
		Epsilon		−6.39	−3.58	
		Terminal		−6.78	−4.20	
PFPiA & PFPA	Bis(nonafluorobutyl)phosphinic acid	Alpha	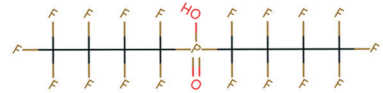	−5.66	−3.11	−2.81
		Beta		−5.77	−3.28	
		Gamma		−5.89	−3.32	
		Terminal		−6.27	−3.74	
	Perfluorohexanephosphonic acid	Alpha	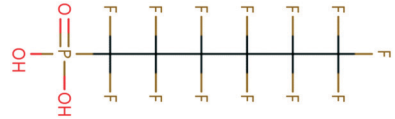	−6.48	−3.40	−3.43
		Beta		−6.40	−3.39	
		Gamma		−6.54	−3.45	
		Delta		−6.47	−3.37	
		Epsilon		−6.44	−3.40	
		Terminal		−6.88	−3.86	
	Perfluorooctanephosphonic acid	Alpha	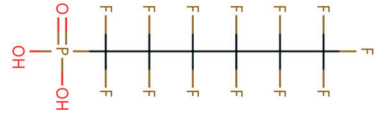	−6.14	−3.33	−3.20
		Beta		−6.12	−3.35	
		Gamma		−6.19	−3.35	
		Delta		−6.11	−3.36	

Table 2 *(continued)*

Class	Compound name	Attacking site	2D structure	E°_{red} (V *vs.* SHE) Stepwise (C–F cleavage)	Concerted (C–F cleavage)	Association with functional group
		Epsilon		−6.27	−3.40	
		Zeta		−6.16	−3.31	
		Eta		−6.18	−3.36	
		Terminal		−6.65	−3.82	
	Perfluorodecylphosphonic acid	Alpha	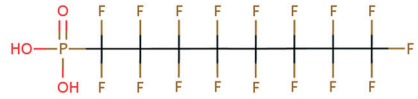	−5.53	−3.54	−3.25
		Beta		−5.51	−3.58	
		Gamma		−5.49	−3.50	
		Delta		−5.53	−3.51	
		Epsilon		−5.61	−3.58	
		Zeta		−5.49	−3.51	
		Eta		−5.50	−3.48	
		Theta		−5.44	−3.45	
		Iota		−5.52	−3.55	
		Terminal		−5.90	−3.96	
	P,Pbis(1,1,2,2,3,3,4,4,5,5,6,6,6-tridecafluorohexyl)-phosphinic acid	Alpha		−5.08	−3.44	−3.05
		Beta		−5.15	−3.44	
		Gamma		−5.22	−3.56	
		Delta		−5.23	−3.54	
		Epsilon		−5.33	−3.64	
		Terminal		−5.65	−4.01	
	(Heptadecafluorooctyl)(tridecafluorohexyl) phosphinic acid	Alpha	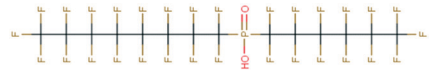	−4.77	−3.36	−3.31
		Beta		−4.95	−3.54	
		Gamma		−4.97	−3.51	
		Delta		−5.02	−3.55	
		Epsilon		−5.03	−3.57	
		Zeta		−4.96	−3.47	
		Terminal		−5.08	−3.61	
	Bis(heptadecafluorooctyl)phosphinic acid	Alpha	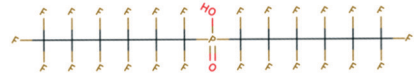	−4.44	−3.46	−3.39
		Beta		−4.52	−3.57	
		Gamma		−4.50	−3.52	
		Delta		−4.43	−3.54	
		Epsilon		−4.50	−3.51	
		Zeta		−4.59	−3.55	
		Eta		−4.70	−3.64	
		Terminal		−4.98	−4.02	
FTOH	4:2 fluorotelomer alcohol	Alpha		−6.86	−3.71	−4.20
		Beta		−6.81	−3.65	
		Gamma		−6.80	−3.64	
		Terminal		−7.14	−4.02	
	6:2 fluorotelomer alcohol	Alpha	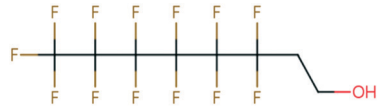	−6.50	−3.56	−3.49
		Beta		−6.45	−3.46	
		Gamma		−6.40	−3.38	
		Delta		−6.32	−3.37	
		Epsilon		−6.39	−3.43	
		Terminal		−6.78	−3.87	

Table 2 *(continued)*

Class	Compound name	Attacking site	2D structure	E°_{red} (V *vs.* SHE) Stepwise (C–F cleavage)	Concerted (C–F cleavage)	Association with functional group
	4:4 fluorotelomer alcohol	Alpha	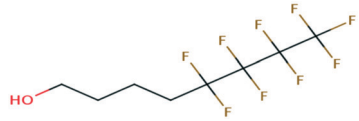	−6.60	−3.68	−3.93
		Beta		—	—	
		Gamma		−6.54	−3.59	
		Terminal		−6.94	−4.03	
	8:2 fluorotelomer alcohol	Alpha		—	—	−3.08
		Beta		−6.07	−3.32	
		Gamma		−6.05	−3.28	
		Delta		−5.92	−3.24	
		Epsilon		−5.92	−3.24	
		Zeta		−5.99	−3.25	
		Eta		−6.08	−3.37	
		Terminal		—	—	
	11:1 fluorotelomer alcohol	Alpha	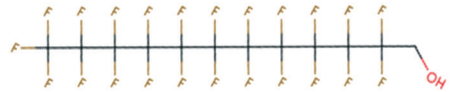	−5.70	−3.20	−3.02
		Beta		−5.68	−3.12	
		Gamma		−5.58	−3.05	
		Delta		−5.54	−3.03	
		Epsilon		−5.55	−3.01	
		Zeta		−5.53	−3.01	
		Eta		−5.57	−3.04	
		Theta		−5.52	−3.01	
		Iota		−5.60	−3.03	
		Kappa		−5.61	−3.09	
		Terminal		—	—	
	Heptafluorobutanol	Alpha	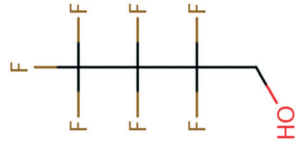	−7.26	−3.75	−3.57
		Beta		−7.24	−3.70	
		Terminal		−7.55	−4.02	
	3-(Perfluoropropyl)propanol	Alpha	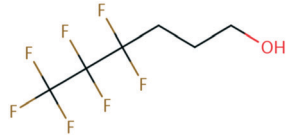	−7.02	−3.68	−2.92
		Beta		−6.97	−3.63	
		Terminal		−7.37	−4.04	
	3-(Perfluoro-2-butyl)propane-1,2-diol	Alpha	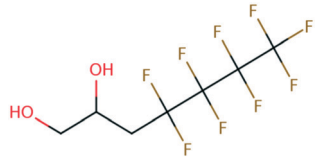	−6.64	−3.69	−3.93
		Beta		−6.57	−3.62	
		Gamma		−6.58	−3.60	
		Terminal		−6.98	−4.04	
Fluorotelomer acrylates (FTACs)	6:2 fluorotelomer acrylate	Alpha	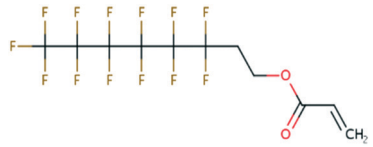	−6.15	−3.55	−2.08
		Beta		−6.13	−3.47	
		Gamma		−6.01	−3.33	
		Delta		−6.09	−3.42	
		Epsilon		−6.13	−3.51	

Table 2 *(continued)*

Class	Compound name	Attacking site	2D structure	E°_{red} (V *vs.* SHE) Stepwise (C–F cleavage)	Concerted (C–F cleavage)	Association with functional group
		Terminal		−6.47	−3.89	
	6:2 fluorotelomer methacrylate	Alpha	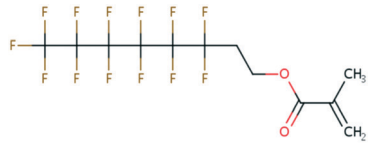	−6.08	−3.71	−1.94
		Beta		−6.03	−3.54	
		Gamma		−5.99	−3.57	
		Delta		−5.95	−3.53	
		Epsilon		−5.97	−3.57	
		Terminal		−6.34	−4.01	
Perfluoroalkyl ether carboxylates (PFECAs)	Perfluoro-2-methyl-3-oxahexanoic acid	Alpha	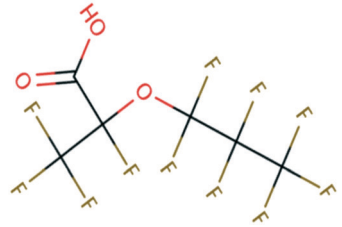	−6.22	−3.42	−3.57
		Beta		−6.88	−4.16	
		Gamma		−6.64	−3.88	
		Delta		−6.28	−3.57	
		Terminal		−6.83	−4.04	
	Perfluoro(4-methoxybutanoic) acid	Alpha	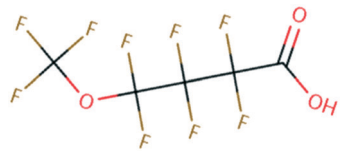	−6.46	−3.36	−3.08
		Beta		−6.67	−3.56	
		Gamma		−6.86	−3.73	
		Terminal		−7.24	−4.17	
	Perfluoro-3,6-dioxaoctane-1,8-dioic acid	Alpha	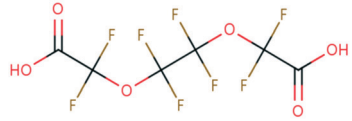	−6.87	−3.71	−3.43
		Terminal		−7.02	−3.82	
FASA	Perfluorooctanesulfonamide	Alpha	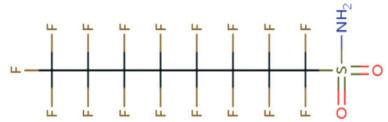	−5.97	−3.54	−1.34
		Beta		−5.92	−3.58	
		Gamma		−5.99	−3.57	
		Delta		−6.03	−3.59	
		Epsilon		−5.91	−3.53	
		Zeta		−6.02	−3.55	
		Eta		−6.06	−3.61	
		Terminal		−6.41	−4.02	
	N-Ethylperfluorooctanesulfonamide	Alpha	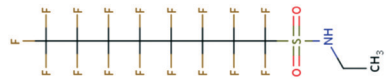	−5.82	−3.57	−1.33
		Beta		−5.73	−3.46	
		Gamma		−5.83	−3.55	
		Delta		−5.76	−3.48	
		Epsilon		−5.85	−3.56	
		Zeta		−5.81	−3.50	
		Eta		−5.88	−3.63	
		Terminal		−6.24	−4.03	
	N-Methylperfluorooctanesulfonamide	Alpha	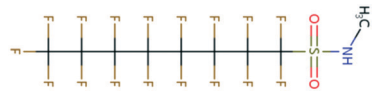	−5.90	−3.62	−1.36
		Beta		−5.80	−3.50	
		Gamma		−5.97	−3.60	

Table 2 *(continued)*

Class	Compound name	Attacking site	2D structure	E°_{red} (V *vs.* SHE) Stepwise (C–F cleavage)	Concerted (C–F cleavage)	Association with functional group
		Delta		−5.86	−3.57	
		Epsilon		−5.95	−3.59	
		Zeta		−5.97	−3.61	
		Eta		−5.94	−3.64	
		Terminal		−6.33	−4.04	
Perfluoroalkane sulfonyl fluorides (PASFs)	Perfluorobutanesulfonyl fluoride	Alpha	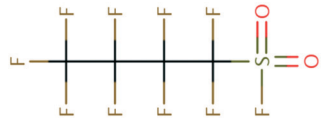	−6.61	−3.50	−0.46
		Beta		−6.58	−3.51	
		Gamma		−6.69	−3.59	
		Terminal		−7.15	−4.12	
Perfluoroalkane sulfonyl chloride (PASCs)	Perfluoro-1-butanesulfonyl chloride	Alpha	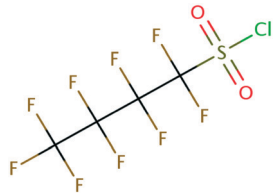	−6.56	−3.54	0.36
		Beta		−6.47	−3.43	
		Gamma		−6.63	−3.55	
		Terminal		−7.10	−4.12	
Perfluoroalkyl acyl fluorides (PAAFs)	Perfluoroglutaryl difluoride	Alpha	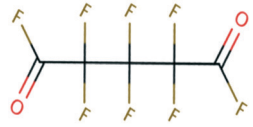	−6.33	−3.13	−1.70
		Beta		−6.83	−3.58	
Fluorotelomer amines	1*H*,1*H*-Perfluoropentylamine	Alpha	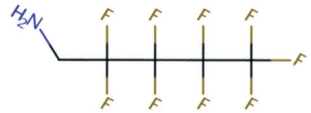	−6.96	−3.73	−3.95
		Beta		−6.85	−3.60	
		Gamma		−6.83	−3.58	
		Terminal		−7.21	−4.02	
	Bis(1*H*,1*H*-perfluoropropyl)amine	Alpha	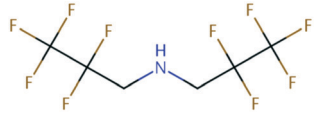	−6.77	−3.75	−4.46
		Terminal		−7.10	−4.12	
Perfluoroalkyl amides	Octafluoroadipamide	Alpha	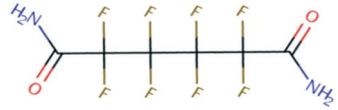	−6.37	−3.42	−2.66
		Beta		−6.55	−3.63	
	Nonafluoropentanamide	Alpha	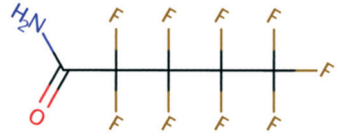	−6.60	−3.45	−2.70
		Beta		−6.77	−3.58	
		Gamma		−6.76	−3.55	
		Terminal		−7.19	−4.04	
	Heptafluorobutyramide	Alpha	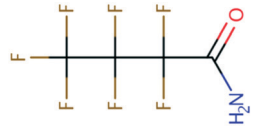	−6.59	−3.18	−2.78
		Beta		−6.87	−3.46	
		Terminal		−7.24	−3.84	

Table 2 *(continued)*

Class	Compound name	Attacking site	2D structure	E°_{red} (V *vs.* SHE) Stepwise (C–F cleavage)	Concerted (C–F cleavage)	Association with functional group
Perfluoroalkyl anhydrides	Pentafluoropropanoic anhydride	Alpha Terminal	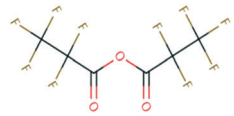	−6.26 −7.12	−3.20 −4.06	−1.35
Polyfluoroalkyl acyl fluorides	5*H*-Octafluoropentanoyl fluoride	Alpha Beta Gamma Terminal	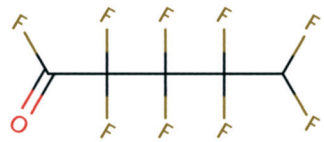	−6.35 −6.80 −6.80 −6.91	−3.17 −3.59 −3.59 −3.72	−1.74
Polyfluoroalkyl aldehydes	5*H*-Perfluoropentanal	Alpha Beta Gamma Terminal	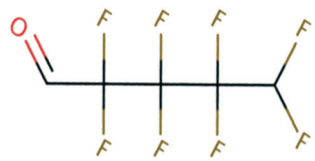	−6.34 −6.81 −6.85 −6.95	−3.13 −3.56 −3.59 −3.73	−1.74
Polyfluoroalkyl ethers	Sevoflurane	Alpha Beta Terminal	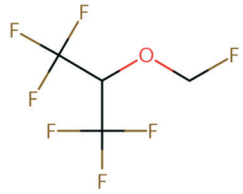	−7.08 −7.48 −7.50	−3.74 −4.12 −4.14	−2.67
	Flurothyl	Terminal	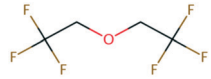	−7.66	−4.14	−3.07
	Perfluoroisobutyl methyl ether	Alpha Beta Gamma Terminal	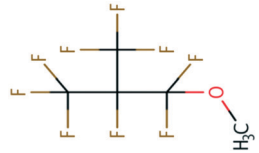	−7.13 −6.46 −7.27 −7.26	−3.89 −3.17 −4.04 −4.02	−2.16
	Tris(trifluoroethoxy)methane	Terminal	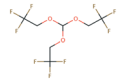	−7.01	−4.21	−4.55
	Difluoromethyl 1*H*,1*H*-perfluoropropyl	Alpha Beta Terminal	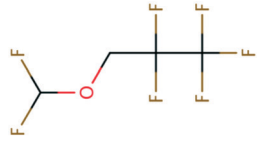	−7.32 −7.03 −7.42	−4.07 −3.69 −4.10	−2.11

Table 2 *(continued)*

Class	Compound name	Attacking site	2D structure	E°_{red} (V *vs.* SHE) Stepwise (C–F cleavage)	Concerted (C–F cleavage)	Association with functional group
	Allyl perfluoroisopropyl ether	Alpha Beta Terminal	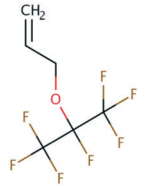	−6.62 −7.30 −7.27	−3.37 −4.07 −4.03	−1.26
Semi-fluorinated alkenes (SFAenes)	1*H*,1*H*,2*H*-Perfluoro-1-hexene	Alpha Beta Gamma Terminal		−6.31 −6.84 −6.89 −7.22	−3.15 −3.62 −3.66 −4.03	−2.67
	6*H*-Perfluorohex-1-ene	Alpha Beta Gamma Delta Epsilon Terminal	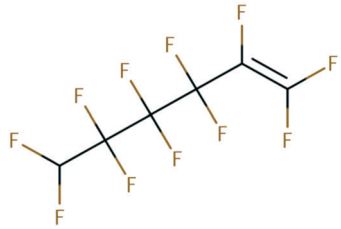	−7.20 −6.79 −6.23 −6.73 −6.66 −6.78	−4.15 −3.76 −3.18 −3.65 −3.56 −3.70	−2.28
	2-Vinylperfluorobutane	Alpha Beta Gamma Terminal	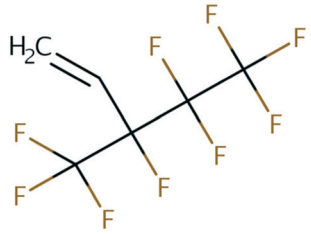	−5.85 −7.32 −6.84 −7.25	−2.66 −4.08 −3.58 −4.02	−2.27
	1-Propenylperfluoropropane	Alpha Beta Terminal	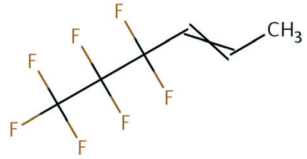	−6.45 −6.95 −7.30	−3.21 −3.66 −4.05	−2.84
Perfluoroalkyl alkyl ethers (PFAEs)	Ethyl perfluorobutyl ether	Alpha Beta Gamma Terminal		−6.97 −6.75 −6.78 −7.08	−3.88 −3.64 −3.66 −4.14	−3.90
Polyfluorinated alcohols	1*H*,1*H*,5*H*-Perfluoropentanol	Alpha Beta Gamma Terminal	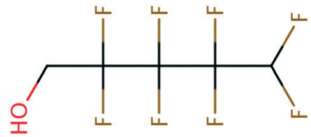	−7.01 −6.89 −6.87 −6.96	−3.71 −3.57 −3.62 −3.73	−2.18

Table 2 *(continued)*

Class	Compound name	Attacking site	2D structure	E°_{red} (V *vs.* SHE) Stepwise (C–F cleavage)	Concerted (C–F cleavage)	Association with functional group
	Dodecafluoroheptanol	Alpha	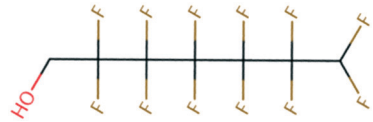	−6.62	−3.72	−3.72
		Beta		−6.61	−3.65	
		Gamma		−6.44	−3.54	
		Delta		−6.58	−3.59	
		Epsilon		−6.55	−3.60	
		Terminal		−6.58	−3.71	
	Hexafluoroamylene glycol	Alpha	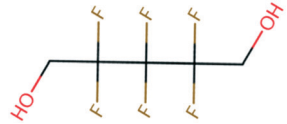	−7.05	−3.66	−2.73
		Beta		−7.04	−3.69	
	3*H*-Perfluoro-2,2,4,4-tetrahydroxypentane	Alpha	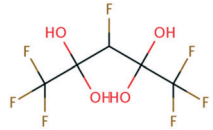	−6.68	−3.51	−2.86
		Terminal		−7.17	−3.96	
	1-Pentafluoroethylethanol	Alpha	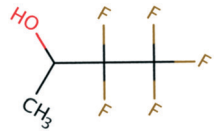	−7.21	−3.72	−4.02
		Terminal		−7.53	−4.08	
Polyfluoroalkyl carboxylates	4*H*-Perfluorobutanoic acid	Alpha	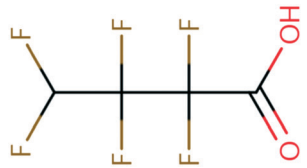	−6.87	−3.51	−3.17
		Beta		−7.11	−3.72	
		Terminal		−7.12	−3.75	
	3,3-Bis(trifluoromethyl)-2-propenoic acid	Alpha	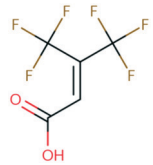	−7.00	−3.65	−2.02
		Terminal		−7.03	−3.67	
	3-(Perfluoroisopropyl)-2-propenoic acid	Alpha	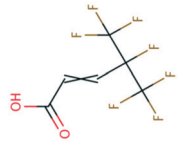	−5.88	−2.58	−2.62
		Terminal		−7.33	−4.01	
Fluorotelomer carboxylates (FTCAs)	2*H*,2*H*,3*H*,3*H*-Perfluorooctanoic acid	Alpha	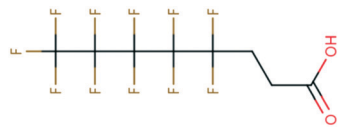	−6.78	−3.59	−3.30
		Beta		−6.72	−3.50	
		Gamma		−6.63	−3.39	
		Delta		−6.65	−3.43	
		Terminal		−7.02	−3.85	

Table 2 *(continued)*

Class	Compound name	Attacking site	2D structure	E°_{red} (V *vs.* SHE) Stepwise (C–F cleavage)	Concerted (C–F cleavage)	Association with functional group
	Methyl 2*H*,2*H*,3*H*,3*H*-perfluoroheptanoate	Alpha	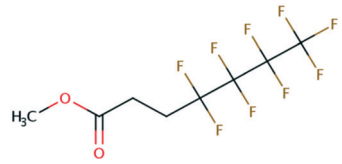	−6.59	−3.71	−3.25
		Beta		−6.51	−3.63	
		Gamma		−6.48	−3.57	
		Terminal		−6.88	−4.03	
Fluorotelomer sulfonates (FTSAs)	4:2 fluorotelomer sulfonic acid	Alpha	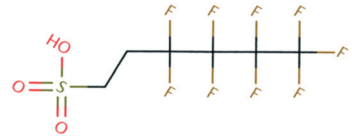	−6.70	−3.77	−2.94
		Beta		−6.58	−3.62	
		Gamma		−6.51	−3.57	
		Terminal		−6.94	−4.04	
N-Alkyl perfluoroalkane sulfonamidoethanols	*N*-Ethyl-*N*-(2-hydroxyethyl) perfluorooctanesulfonamide	Alpha	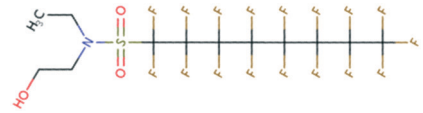	−5.58	−3.58	−1.25
		Beta		−5.45	−3.48	
		Gamma		−5.60	−3.56	
		Delta		−5.57	−3.56	
		Epsilon		−5.64	−3.58	
		Zeta		−5.68	−3.58	
		Eta		−5.62	−3.62	
		Terminal		−5.99	−4.02	
Perfluoroalkyl polyether carboxylates (PFPECAs)	Perfluoro-3,6,9-trioxatridecanoic acid	Alpha	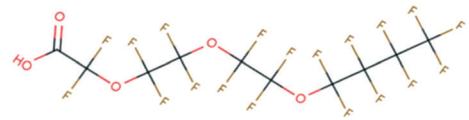	−6.13	−3.48	−1.51
		Beta		−6.28	−3.57	
		Gamma		−6.31	−3.59	
		Delta		−6.29	−3.58	
		Epsilon		−6.36	−3.61	
		Zeta		−6.19	−3.45	
		Eta		−6.00	−3.28	
		Theta		−6.02	−3.30	
		Terminal		−6.41	−3.73	
	Perfluoro-3,6-dioxaheptanoic acid	Alpha	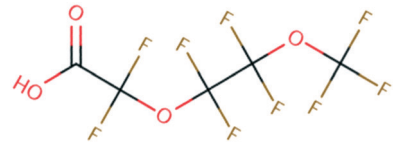	−6.75	−3.58	−3.39
		Beta		−6.93	−3.72	
		Gamma		−6.90	−3.67	
		Terminal		−7.29	−4.09	
Perfluoroalkyl sulfonamido amines	Perfluorooctanesulfonamido ammonium iodide	Alpha	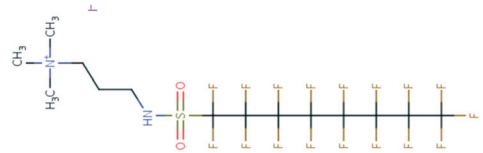	−5.57	−3.65	−1.24
		Beta		−5.20	−3.43	
		Gamma		−5.27	−3.45	
		Delta		−5.23	−3.41	
		Epsilon		−5.34	−3.49	
		Zeta		−5.43	−3.51	
		Eta		−5.51	−3.62	
		Terminal		−5.85	−4.05	

Table 2 *(continued)*

Class	Compound name	Attacking site	2D structure	E°_{red} (V *vs.* SHE) Stepwise (C–F cleavage)	Concerted (C–F cleavage)	Association with functional group
Perfluoroalkyl aldehydes (PFALs)	Perfluorobutyraldehyde	Alpha Beta Terminal	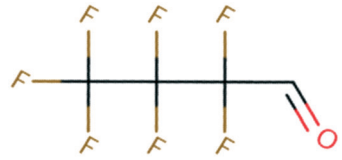	−6.45 −7.01 −7.43	−3.02 −3.51 −3.96	−1.56
Perfluoroalkyl amino alcohols	2-Aminohexafluoropropan-2-ol	Alpha Terminal	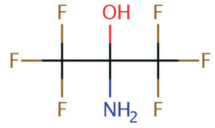	−7.60 −7.60	−4.12 −4.13	−3.63
Perfluoroalkyl Ketones	Methyl perfluoroethyl ketone	Alpha Terminal	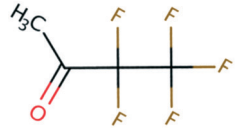	−6.73 −7.54	−3.25 −4.07	−2.05
Perfluoroalkyl polyether alcohols	1*H*,1*H*,8*H*,8*H*-Perfluoro-3,6-dioxaoctane-1,8-diol	Alpha Terminal	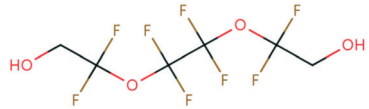	−6.92 −6.81	−4.00 −3.87	−1.77
Perfluoroalkyl vinyl ethers	Heptafluoropropyl trifluorovinyl ether	Alpha Beta Gamma Delta Terminal	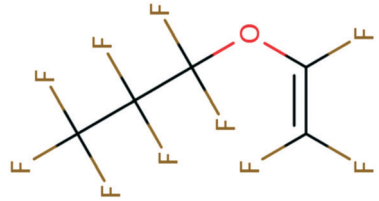	−7.40 −7.14 −7.16 −6.83 −7.23	−3.97 −3.69 −3.62 −3.36 −3.77	−3.57
Polyfluoroalkane sulfonates	2,2-Difluoroethyl triflate	Alpha Terminal	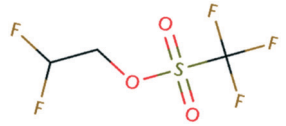	−7.28 −7.05	−3.95 −3.74	−1.11
Polyfluoroalkyl amides	Perfluoropentanamide	Alpha Beta Gamma Terminal	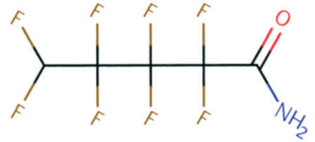	−6.63 −6.77 −6.77 −6.89	−3.46 −3.60 −3.57 −3.72	−2.78
Polyfluoroalkyl Amines	2-Amino-2*H*-perfluoropropane	Terminal	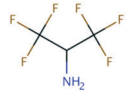	−7.68	−4.16	−4.24

Table 2 *(continued)*

Class	Compound name	Attacking site	2D structure	E°_{red} (V *vs.* SHE)		Association with functional group
				Stepwise (C–F cleavage)	Concerted (C–F cleavage)	
Polyfluoroalkyl ketones	3*H*-Perfluoro-4-hydroxy-3-penten-2-one	Alpha	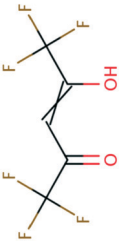	−6.88	−3.56	−1.20
		Terminal		−6.86	−3.52	
Polyfluoroalkyl trifluoromethane-sulfonates	2-(Trifluoromethoxy)ethyl trifluoromethanesulfonate	Alpha	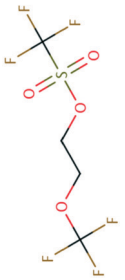	−7.10	−3.96	−0.58
		Terminal		−7.34	−4.09	
Semi-fluorinated alkanes (SFAs)	1,1,1,3,3-Pentafluorobutane	Alpha	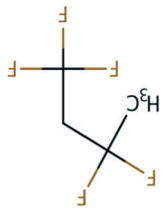	−7.48	−3.79	−4.94
		Terminal		−7.86	−4.16	

with O, and $4k_{chem}$ values are above the diffusion limit for the C=C associative mechanism. We did not determine the LFERs for the functional groups of sulfonic acid (SO_3^-), phosphinic acid ($PO(OH)_2$), sulfonamide (SO_2NH), and sulfonyl (SO_2); thus, no rate constant predictions were conducted. The investigation of the $E^{\circ}_{red,aq}$ values at all possible e_{aq}^- attacking sites for all possible e_{aq}^- reaction mechanisms highlights the significantly lower reactivity of e_{aq}^- for the stepwise cleavage mechanism of a C–F bond and higher reactivity of e_{aq}^- with functional groups in a given PFAS structure.

The attachment of an e_{aq}^- to the group of PFCAs (N = 8) occurred near the α-carbon, and the resultant intermediate radical dianions were the most stable due to resonance stabilization by the π-system of carboxylate functional groups, which is consistent with previous predictions on PFOA[163] and perfluoropentanoic acid (PFPeA).[24] Attachment near the α-carbon was also observed for the group of perfluoroalkyl phosphinates (PFPiAs) due to the phosphonate functional group, perfluoroalkyl ether carboxylates (PFECA), perfluoroalkyl amides, polyfluoroalkyl aldehydes and acyl fluorides, and semifluorinated alkenes (SFAenes). In contrast, the group of perfluoroalkane sulfonates (PFSA) (N = 5) showed preferable attachment of an e_{aq}^- near the β- or γ-carbon with the largest $E^{\circ}_{red,aq}$ values due to the inability of π-stabilization due to the trigonal geometry of the sulfonate functional group.[24] A similar trend was observed for the groups of fluorotelomer alcohols (FTOH) and polyfluorinated alcohols, fluorotelomer acrylates (FTACs), perfluoroalkane sulfonamides (FASAs), perfluoroalkane sulfonyl chlorides (PASCs), and fluorotelomer carboxylates (FTCAs). The investigation of the $E^{\circ}_{red,aq}$ values at all possible e_{aq}^- attacking sites for PFASs that contain a wide variety of functional groups highlights significant differences in regard to the most preferable reactive sites of e_{aq}^-. While the scope of the current study is on the initial reactivities of e_{aq}^- with a wide variety of organic compounds and PFASs, investigating the subsequent degradation pathways is underway. The cleavage of a C–F bond in a PFAS is the major goal for practical PFAS remediation using reductive technologies, and our LFERs and predicted k_{chem} values for the stepwise cleavage mechanism of a C–F bond present significant challenges in cleaving a C–F bond from a kinetics point of view.

Impact of the accuracy of rate constant estimation to the fate

To assess the impact of the accuracy of rate constant estimation to the fate of a target organic compound, we develop an unsteady-state kinetic model for the homogeneous aqueous-phase UV/sulfite system to degrade a model compound (*e.g.*, PFAS) with input parameters that are consistent with experimental observations in the literature[10] (see the details in Text S4 in the ESI†). It should be noted that the model was used to assess the impact of the initial rate constant prediction accuracy on the time-dependent fate

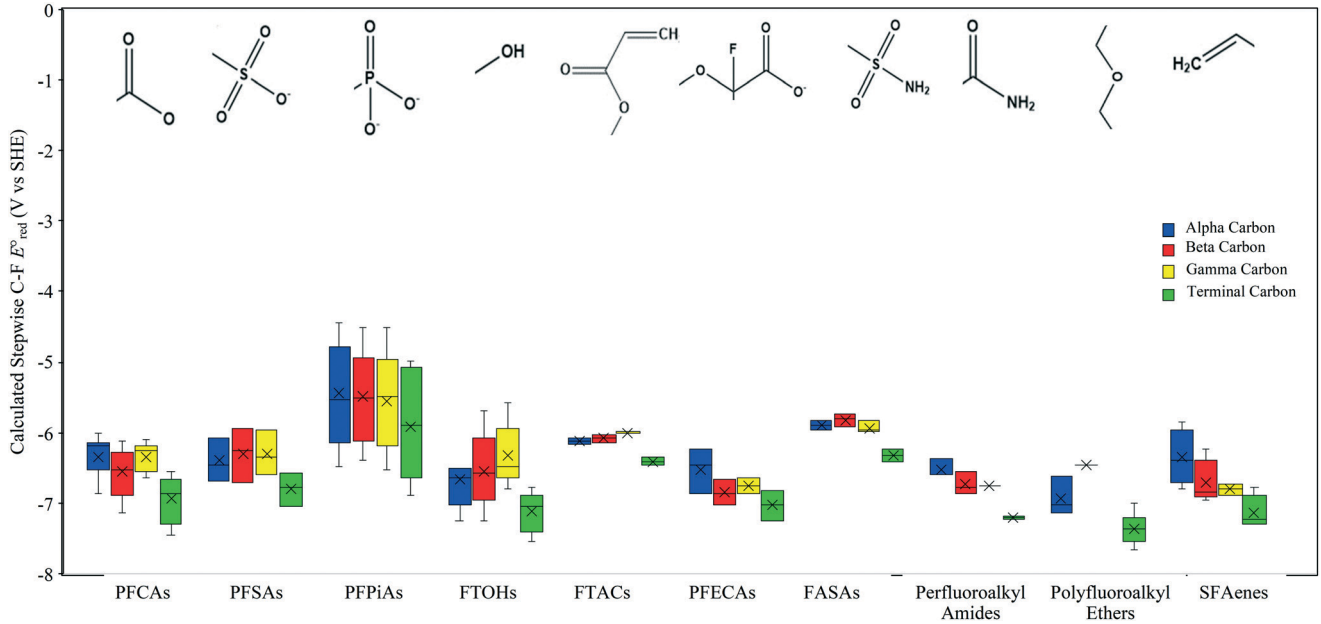

Fig. 4 Theoretically calculated $E^{\circ}_{red,aq}$ values for the cleavage of a C–F bond at different positions of various PFASs. The $E^{\circ}_{red,aq}$ values were calculated based on M06-2X/cc-pVDZ.

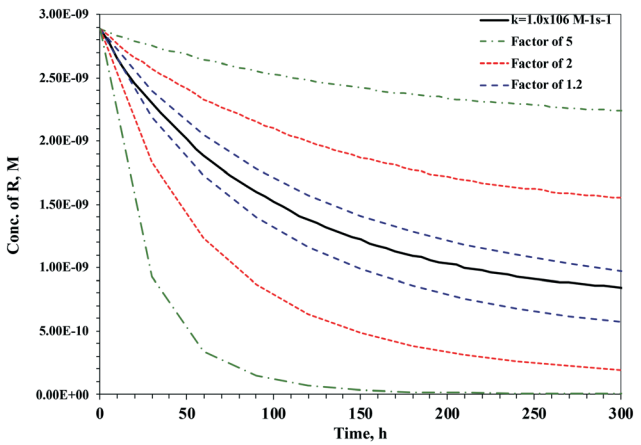

Fig. 5 Time-dependent concentration of a target compound with k_{chem} = 1.0 × 10^6 M^{-1} s^{-1} and different predicted values by a difference of a factor of 1.2, 2, and 5 in UV/sulfite process.[10]

and the predicted results do not necessarily indicate the degradation of a model compound in an environmental matrix. Fig. 5 represents the time-dependent concentration profile of a parent compound that has k_{chem} = 1.0 × 10^6 M^{-1} s^{-1} with e_{aq}^-. The profiles were also predicted by changing the k_{chem} values by a difference of a factor of 1.2, 2, and 5. Estimating the rate constant impacted the profile of the parent compound by 33% for k_{chem} values with a factor of 1.2, 77% with a factor of 2, and 100% with a factor of 5.0 at 300 h. While our LFER for the C–F stepwise cleavage mechanism has the ability to predict the k_{chem} values within the difference of a factor of 1.2, this prediction demonstrates the importance of an accurate rate constant of a target compound in estimating the decay of an environmentally relevant contaminant that requires significant amount of time (*e.g.*, PFASs).

Conclusion

Reduction of oxidized forms of water contaminants using electrons in the aqueous-phase advanced reduction processes is a novel and attractive approach to destroying the contaminants. The mechanistic insight into the reactivities of solvated electrons with a wide variety of contaminants helps understand and predict the fate of contaminants of emerging concern, and can be extrapolated to the direct electron transfer mechanisms in the heterogeneous electrochemical processes. The determination of linear free energy relationships presented in this study elucidated which reaction mechanisms are the dominant rate-determining step for the reaction of solvated electrons with structurally diverse conventional organic compounds and the 75 priority PFAS subset that contains a wide variety of functional groups. The computational tools determined in this study can be used to predict the reaction rate constants with solvated electrons and screen a number of contaminants and prioritize for the application of advanced reduction processes.

Conflicts of interest

There are no conflicts to declare.

Acknowledgements

This work was supported by Central Chemicals Inc. Any opinions, findings, conclusions, or recommendations expressed in this publication are those of the authors and

do not necessarily reflect the view of the supporting organization. R. D. is supported by the NSF Graduate Research Fellowship Program (GRFP). The authors appreciate the support for the use of the Michigan Tech HPC cluster 'Superior'.

References

1 W. Glaze, J.-W. Kang and H. Chapin, The chemistry of water treatment processes involving ozone, hydrogen peroxide and ultraviolet radiation, *Ozone: Sci. Eng.*, 1987, **9**, 335–352.
2 W. Glaze and J.-W. Kang, Advanced oxidation processes. Test of a kinetic model for the oxidation of organic compounds with ozone and hydrogen peroxide in a semibatch reactor, *Ind. Eng. Chem. Res.*, 1989, **28**, 1580–1587.
3 C. Remucal and D. Manley, Emerging investigators series: the efficacy of chlorine photolysis as an advanced oxidation process for drinking water treatment, *Environ. Sci.: Water Res. Technol.*, 2016, **2**, 565–579.
4 D. Minakata, D. Kamath and S. Maetzold, Mechanistic insight into the reactivity of chlorine-derived radicals in the aqueous-phase UV-chlorine advanced oxidation process: Quantum mechanical calculations, *Environ. Sci. Technol.*, 2017, **51**, 6918–6926.
5 K. Guo, S. Zheng, X. Zhang, L. Zhao, S. Ji, C. Chen, Z. Wu, D. Wang and J. Fang, Roles of bromine radicals and hydroxyl radicals in the degradation of micropollutants by the UV/bromine process, *Environ. Sci. Technol.*, 2020, **54**, 6415–6426.
6 Z. Wu, C. Chen, B.-Z. Zhu, C.-H. Huang, T. An, F. Meng and J. Fang, Reactive nitrogen species are also involved in the transformation of micropollutants by the UV/monochloramine process, *Environ. Sci. Technol.*, 2019, **53**, 11142–11152.
7 B. Vellanki, B. Batchelor and A. Abdel-Wahab, Advanced reduction processes: A new class of treatment processes, *Environ. Eng. Sci.*, 2013, **30**, 264–271.
8 J. Grebel, J. Pignatello and W. Mitch, Effect of halide ions and carbonates on organic contaminant degradation by hydroxyl radical-based advanced oxidation processes in saline waters, *Environ. Sci. Technol.*, 2010, **44**, 6822–6828.
9 X. Li, J. Ma, G. Liu, J. Fang, S. Yue, Y. Guan, L. Chen and X. Liu, Efficient reductive dechlorination of monochloroacetic acid by sulfite/UV process, *Environ. Sci. Technol.*, 2012, **46**, 7342–7349.
10 R. Tenorio, J. Liu, X. Xiao, A. Maizel, C. Higgins, C. Schaefer and T. Strathmann, Destruction of per- and polyfluoroalkyl substances (PFASs) in aqueous film-forming foam (AFFF) with UV-sulfite photoreductive treatment, *Environ. Sci. Technol.*, 2020, **54**, 6957–6967.
11 E. Mousset and K. Doudrick, A review of electrochemical reduction processes to treat oxidized contaminants in water, *Curr. Opin. Electrochem.*, 2020, **22**, 221–227.
12 C. Zhang, D. He, J. Ma, W. Tang and T. Waite, Faradic reactions in capacitive deionization (CDI) – problems and possibilities: A review, *Water Res.*, 2018, **128**, 314–330.
13 Y. Su, U. Rao, C. Khor, M. Jensen, L. Teesch, B. Wong, D. Cwiertny and D. Jassby, Potential-driven electron transfer lowers the dissociation energy of the C-F bond and facilitates reductive defluorination of perfluorooctane sulfonate (PFOS), *ACS Appl. Mater. Interfaces*, 2019, **11**, 33913–33922.
14 Y. Wang and P. Zhang, Photocatalytic decomposition of perfluorooctanoic acid (PFOA) by TiO2 in the presence of oxalic acid, *J. Hazard. Mater.*, 2011, **192**, 1869–1875.
15 J. Cui, P. Gao and Y. Deng, Destruction of per- and polyfluoroalkyl substance (PFAS) with advanced reduction processes (ARPs): A critical review, *Environ. Sci. Technol.*, 2020, **54**, 3752–3766.
16 P. Tentscher, M. Lee and U. von Gunten, Micropollutant oxidation studied by quantum chemical computations: Methodology and applications to thermodynamics, kinetics, and reaction mechanisms, *Acc. Chem. Res.*, 2019, **52**, 605–614.
17 *NDRL/NIST Solution Kinetics Database on the Web, NIST Standard Reference Database 40*, https://kinetics.nist.gov/solution/, (accessed August 2021).
18 C. Li, S. Zheng, T. Li, J. Chen, J. Zhou, L. Su, Y.-N. Zhang, J. Crittenden, S. Zhu and Y. Zhao, Quantitative structure-activity relationship models for predicting reaction rate constants of organic contaminants with hydrated electrons and their mechanistic pathways, *Water Res.*, 2019, **151**, 468–477.
19 S. Zheng, C. Li and G. Wei, QSAR modeling for reaction rate constants of e_{aq}^- with diverse organic compounds in water, *Environ. Sci.: Water Res. Technol.*, 2020, **6**, 1931–1938.
20 E. Hart, J. Thomas and S. Gordon, A review of the radiation chemistry of single-carbon compounds and some reactions of the hydrated electrons in aqueous solution, *Radiat. Res., Suppl.*, 1964, **4**, 75–88.
21 E. Bylaska, M. Dupuis and P. Tratnyek, Ab initio electronic structure study of one-electron reduction of polychlorinated ethylenes, *J. Phys. Chem. A*, 2005, **109**, 5905–5916.
22 E. Bylaska, M. Dupuis and P. Tratneyk, One-electron-transfer reactions of polychlorinated ethylenes: Concerted and stepwise cleavages, *J. Phys. Chem. A*, 2008, **112**, 3712–3721.
23 S. Rosokha, E. Lukacs, J. Ritzert and A. Wasilewki, Mechanism and thermodynamics of reductive cleavage of carbon-halogen bonds in the polybrominated aliphatic electrophiles, *J. Phys. Chem. A*, 2016, **120**, 1706–1715.
24 D. Van Hoomissen and S. Vyas, Early events in the reductive dehalogenation of linear perfluoroalkyl substances, *Environ. Sci. Technol. Lett.*, 2019, **6**, 365–371.
25 Y. Zhang, A. Moores, J. Liu and S. Ghoshal, New insights into the degradation mechanism of perfluorooctanoic acid by persulfate from density functional theory and experimental data, *Environ. Sci. Technol.*, 2019, **53**, 8672–8681.
26 A. Carre-Burritt, D. Van Hoomissen and S. Vyas, Role of pH in the transformation of perfluoroalkyl carboxylic acids by activated persulfate: Implications from the determination

of absolute electron-transfer rates and chemical computations, *Environ. Sci. Technol.*, 2021, **55**, 8928–8936.

27 G. Patlewicz, A. Richard, A. Williams, C. Grulke, R. Sams, J. Lambert, P. Noyes, M. DeVito, R. Hines, M. Strynar, A. Guiseppi-Elie and R. Thomas, A chemical category-based prioritization approach for selecting 75 per- and polyfluoroalkyl substances (PFAS) for tiered toxicity and toxicokinetic testing, *Environ. Health Perspect.*, 2019, **127**, 014501.

28 S. Eldin and W. Jencks, Concerted bimolecular substitution reactions of anilino thioethers, *J. Am. Chem. Soc.*, 1995, **117**, 9415–9418.

29 C. Andrieux, J.-M. Savéant, A. Tallec, R. Tardivel and C. Tardy, Concerted and stepwise dissociative electron transfers. Oxidability of the leaving group and strength of the breaking illustrated by the electrochemical reduction of a – substituted acetophenones, *J. Am. Chem. Soc.*, 1997, **119**, 2420–2429.

30 J. Jaworski, M. Cembor and D. Kuck, Solvent effect on reductive bond cleavage of 1-chloro-10-methyltribenzotriquinacene: change from the concerted to the stepwise mechanism, *Electrochim. Acta*, 2007, **52**, 2196–2202.

31 P. Brezonik, *Chemical Kinetics and Process Dynamics in Aquatic Systems*, CRC Press, 1993.

32 A. Isse, C. Lin, M. Coote and A. Gennaro, Estimation of standard reduction potentials of halogen atoms and alkyl halides, *J. Phys. Chem. B*, 2011, **115**, 678–684.

33 Y. Zhao and D. Truhlar, The M06 suite of density functionals for main group thermochemistry, thermochemical kinetics, noncovalent interactions, excited states, and transition elements: two new functionals and systematic testing of four M06-class functionals and 12 other functionals, *Theor. Chem. Acc.*, 2008, **120**, 215–241.

34 A. Bauza, I. Alkorta, A. Frontera and J. Elguero, On the reliability of pure and hybrid DFT methods for the evaluation of halogen, chalcogen, and pnicogen bonds involving anionic and neutral electron donors, *J. Chem. Theory Comput.*, 2013, **9**, 5201–5210.

35 A. V. Marenich, C. J. Cramer and D. G. Truhlar, Universal Solvation Model Based on Solute Electron Density and on a Continuum Model of the Solvent Defined by the Bulk Dielectric Constant and Atomic Surface Tensions, *J. Phys. Chem. B*, 2009, **113**, 6378–6396.

36 M. J. Frisch, *GAUSSIAN 16 (Revision D.01)*, Gaussian Inc., Wallingford, CT, 2016.

37 E. J. Hart, E. M. Fielden and M. Anbar, Reactions of carbonylic compounds with hydrated electrons, *J. Phys. Chem.*, 1967, **71**, 3993–3998.

38 D. Minakata, S. P. Mezyk, J. W. Jones, B. R. Daws and J. C. Crittenden, Development of linear free energy relationships for aqueous phase radical-involved chemical reactions, *Environ. Sci. Technol.*, 2014, **48**, 13925–13932.

39 E. J. Hart, S. Gordon and J. K. Thomas, The Activation Energy of Hydrated Electron Reactions, *J. Phys. Chem.*, 1964, **68**, 1271–1274.

40 N. Getoff, Radiation- and photoinduced degradation of pollutants in water. A comparative study, *Radiat. Phys. Chem.*, 1991, **37**, 673–680.

41 H. A. Schwarz, Reaction of the Hydrated Electron with Water, *J. Phys. Chem.*, 1992, **96**, 8937–8941.

42 D. R. Prasad, M. Z. Hoffman, Q. G. Mulazzani and M. A. Rodgers, Pulsed-Laser Flash and Continuous Photolysis of Aqueous Solutions of Methyl Viologen, Oxalate, and Their Ion-Pair Complexes, *J. Am. Chem. Soc.*, 1986, **108**, 5135–5142.

43 Q. G. Mulazzani, M. D'Angelantonio, M. Venturi, M. Z. Hoffman and M. A. J. Rodgers, Interaction of Formate and Oxalate Ions with Radiation-Generated Radicals in Aqueous Solution. Methylviologen as a Mechanistic Probe, *J. Phys. Chem.*, 1986, **90**, 5347–5352.

44 N. Getoff, S. Schworer, V. M. Markovic, K. Sehested and S. O. Nielsen, Pulse Radiolysis of Oxalic Acid and Oxalates, *J. Phys. Chem.*, 1971, **75**, 749–755.

45 S. Gordon, E. J. Hart, M. S. Matheson and J. Rabani, Reactions of the Hydrated Electron, *Discuss. Faraday Soc.*, 1963, **36**, 193–205.

46 F. A. Peter and P. Neta, The Effect of Ionic Dissociation of Organic Compounds on Their Rate of Reaction with Hydrated Electrons, *J. Phys. Chem.*, 1972, **76**, 630–635.

47 G. Köhler, S. Solar, N. Getoff, A. R. Holzwarth and K. Schaffner, Relationship between the quantum yields of electron photoejection and fluorescence of aromatic carboxylate anions in aqueous solution, *J. Photochem.*, 1985, **28**, 383–391.

48 G. Duplatre and C. D. Jonah, Reactions of electrons in high-concentration water solutions – A comparison between pulse-radiolysis and positron annihilation lifetime spectroscopy data, *Radiat. Phys. Chem.*, 1984, **24**, 557–565.

49 J. A. Bell, E. Grunwald and E. Hayon, Kinetics of Deprotonation of Organic Free Radical in Water. Reaction of $HOCHCO_2^-$, $HOCHCONH_2$, and $HOCCH_3CONH_2$ with Various Bases, *J. Am. Chem. Soc.*, 1975, **97**, 2995–3000.

50 G. O. Phillips and N. W. Worthington, Effects of Ionizing Radiations on Glucuronic Acid, *Radiat. Res.*, 1970, **43**, 34–44.

51 J. A. D. Stockdale and D. F. Sangster, Relative Reaction Rates of Hydrated Electrons with Krebs Cycle and Other Anions, *J. Am. Chem. Soc.*, 1966, **88**, 2907–2910.

52 O. Micic and I. Draganic, Some reactions of hydrated electrons in acid medium (pH 0.6-4.0), *Int. J. Radiat. Phys. Chem.*, 1969, **1**, 287–295.

53 O. I. Micic and V. Markovic, Rates of hydrated electron reactions with undissociated carboxylic acids, *Int. J. Radiat. Phys. Chem.*, 1972, **4**, 43–49.

54 D. Razem and W. H. Hamill, Electron Scavenging in Ethanol and in Water, *J. Phys. Chem.*, 1977, **81**, 1625–1631.

55 S. Castillo-Rojas, A. Negron-Mendoza, Z. D. Draganic and I. G. Draganic, The radiolysis of aqueous solutions of malic acid, *Radiat. Phys. Chem.*, 1985, **26**, 437–443.

56 V. Markovic and K. Sehested, Radiolysis of Aqueous Solutions of Some Simple Compounds Containing

Aldehyde Groups: Part I: Formaldehyde, *Proceedings of the 3. Tihany Symposium on Radiation Chemistry*, 1972, vol. 2, pp. 1243–1253.

57 K. G. Kemsley, J. S. Moore and G. O. Phillips, The effect of molecular size on the rate constants for reaction of hydrated electrons and hydroxyl radicals with carbohydrates, *Int. J. Radiat. Biol. Relat. Stud. Phys. Chem. Med.*, 1979, **36**, 429–432.

58 J. V. Davies, W. Griffiths and G. O. Philips, Pulse radiolysis of aqueous carbohydrate solutions, *Pulse Radiolysis*, 1965, 181–191.

59 M. T. Nenadovic and O. I. Micic, Pulse radiolysis of methyl acetate in aqueous solution, *Radiat. Phys. Chem.*, 1978, **12**, 85–89.

60 A. Biro and L. Wojnarovits, Pulse radiolysis of ethyl propionate in aqueous solution, *J. Radioanal. Nucl. Chem.*, 1992, **166**, 7–14.

61 T. Matsushige, G. Koltzenbur and D. Schulte-Frohlinde, Pulse radiolysis of aqueous solutions of acetic acid 2-hydroxylethyl ester. Fast elimination of acetic acid from a primary radical, *Ber. Bunsen-Ges.*, 1975, **79**, 657–661.

62 W. Bors, D. Tait, C. Michel, M. Saran and M. Erben-Russ, Reactions of Alkoxy Radicals in Aqueous Solution, *Isr. J. Chem.*, 1984, **24**, 17–24.

63 B. Massaut and B. Tilquin, *Reactivity of the "capto-dative" methylmethoxyacetate (MMA) toward radicals, studied by electron pulse radiolysis in neutral aqueous medium*, Belgian Chemical Societies, 1988, vol. 97, pp. 1031–1036.

64 R. L. S. Willix and W. M. Garrison, Chemistry of the hydrated electron in oxygen-free solutions of amino acids, peptides, and related compounds, *Radiat. Res.*, 1967, **32**, 452–462.

65 M. Simic and E. Hayon, Intermediates produced from the one-electron oxidation and reduction of hydroxylamines. Acid-base properties of the amino, hydroxyamino, and methoxyamino radicals, *J. Am. Chem. Soc.*, 1971, **93**, 5982–5986.

66 C. C. Lai and G. R. Freeman, Solvent effects on the reactivity of solvated electrons with organic solutes in methanol/water and ethanol/water mixed solvents, *J. Phys. Chem.*, 1990, **94**, 302–308.

67 G. V. Buxton, C. L. Greenstock, W. P. Helman and A. B. Ross, Critical review of rate constants for reactions of hydrated electrons, hydrogen atoms and hydroxyl radicals ($\cdot OH/\cdot O^-$) in aqueous solution, *J. Phys. Chem. Ref. Data*, 1988, **17**, 513–886.

68 A. M. Afanassiev, K. Okazaki and G. R. Freeman, Effect of Solvation Energy on Electron Reaction Rates in Hydroxylic Solvents, *J. Phys. Chem.*, 1979, **83**, 1244–1249.

69 M. Anbar and E. J. Hart, The Reactivity of Metal Ions and Some Oxy Anions toward Hydrated Electrons, *J. Phys. Chem.*, 1965, **69**, 973–977.

70 K. M. Idriss-Ali and G. R. Freeman, Electron behavior in mixed solvents: optical spectra and reactivities in water/alkane diols, *Can. J. Chem.*, 1984, **62**, 2217–2222.

71 S. P. Mezyk, Rate constant and activation energy determination for reaction of $e^-_{(aq)}$ and ·OH with 2-butanone and propanal, *Can. J. Chem.*, 1994, **72**, 1116–1119.

72 J. Lilie, G. Beck and A. Henglein, Pulsradiolytische Untersuchung des Acetoinradikals und des Diacetylanions in waessriger Loesung, *Ber. Bunsen-Ges.*, 1968, **72**, 529–533.

73 M. Anbar and E. J. Hart, The Activation Energy of Hydrated Electron Reactions, *J. Phys. Chem.*, 1967, **71**, 3700–3702.

74 M. Anbar, Z. B. Alfassi and H. Bregman-Reisler, Hydrated Electron Reactions in View of Their Temperature Dependence, *J. Am. Chem. Soc.*, 1967, **89**, 1263–1264.

75 J. V. Davies, M. Ebert and M. Quintiliani, *Fast intermediate reactions sensitizing alcohol dehydrogenase to radiation*, Taylor and Francis, New York NY, 1970.

76 K. H. Schmidt, P. Han and D. M. Bartels, Radiolytic Yields of the Hydrated Electron from Transient Conductivity. Improved Calculation of the Hydrated Electron Diffusion Coefficient and Analysis of Some Diffusion-Limited (e-)aq Reaction Rates, *J. Phys. Chem.*, 1995, **99**, 10530–10539.

77 N. Getoff, Advancements of Radiation Induced Degradation of Pollutants in Drinking and Waste Water, *Appl. Radiat. Isot.*, 1989, **40**, 585–594.

78 T. I. Balkas, J. H. Fendler and R. H. Schuler, Radiolysis of aqueous solutions of methyl chloride. The concentration dependence for scavenging electrons within spurs, *J. Phys. Chem.*, 1970, **74**, 4497–4505.

79 D. Hayes, K. H. Schmidt and D. Meisel, Growth mechanisms of silver halide clusters from the molecule to the colloidal particle, *J. Phys. Chem.*, 1989, **93**, 6100–6109.

80 M. Lal and H. S. Mahal, Reactions of alkylbromides with free radicals in aqueous solutions, *Radiat. Phys. Chem.*, 1992, **40**, 23–26.

81 G. Bullock and R. Cooper, Reactions of Aqueous Trifluoromethyl Radicals, *Trans. Faraday Soc.*, 1970, **66**, 2055–2064.

82 A. Szutka, J. K. Thomas, S. Gordon and E. J. Hart, Rate Constants of Hydrated Electron Reactions with Some Aromatic Acids, Alkyl Halides, Heterocyclic Compounds, and Werner Complexes, *J. Phys. Chem.*, 1965, **69**, 289–292.

83 J. Monig, K. Asmus, M. Schaeffer, T. F. Slater and R. L. Willson, Electron transfer reactions of halothane-derived peroxyl free radicals, $CF_3CHClO_2\cdot$: Measurement of absolute rate constants by pulse radiolysis, *J. Chem. Soc., Perkin Trans. 2*, 1983, 1133–1137.

84 M. Lal, C. Schoneich, J. Monig and K. Asmus, Rate constants for the reactions of halogenated organic radicals, *Int. J. Radiat. Biol.*, 1988, **54**, 773–785.

85 P. P. Infelta, M. Gratzel and J. K. Thomas, Luminescence Decay of Hydrophobic Molecules Solubilized in Aqueous Micellar Systems. A Kinetic Model, *J. Phys. Chem.*, 1974, **78**, 190–195.

86 T. I. Balkas, The radiolysis of aqueous solutions of methylene chloride, *Int. J. Radiat. Phys. Chem.*, 1972, **4**, 199–208.

87 T. I. Balkas, J. H. Fendler and R. H. Schuler, The radiation chemistry of aqueous solutions of $CFCl_3$, CF_2Cl_2, and CF_3Cl, *J. Phys. Chem.*, 1971, **75**, 455–466.

88 O. I. Micic and B. Cercek, Diffusion-Controlled Reactions in Mixed Solvents, *J. Phys. Chem.*, 1977, **81**, 833–837.
89 I. M. Salih, T. Soeylemez and T. I. Balkas, Radiolysis of aqueous solutions of difluorochloromethane, *Radiat. Res.*, 1976, **67**, 235–243.
90 N. Getoff, Decomposition of biological resistant pollutants in water by irradiation, *Radiat. Phys. Chem.*, 1990, **35**, 432–439.
91 J. K. Thomas, Pulse radiolysis of aqueous solutions of methyl iodide and methyl bromide. The reactions of iodine atoms and methyl radicals in water, *J. Phys. Chem.*, 1967, **71**, 1919–1925.
92 J. L. Faria and S. Steenken, Photoionization (.lambda. = 248 or 308 nm) of triphenylmethyl radical in aqueous solution. Formation of triphenylmethyl carbocation, *J. Am. Chem. Soc.*, 1990, **112**, 1277–1279.
93 E. Hayon and A. O. Allen, Evidence for two kinds of "H atoms" in the radiation chemistry of water, *J. Phys. Chem.*, 1961, **65**, 2181–2185.
94 T. Eriksen, A. Henglein and K. Stockhausen, Pulse radiolytic oxidation of chloral hydrate in oxygenated and deoxygenated aqueous solutions, *J. Chem. Soc., Faraday Trans. 1*, 1973, **69**, 337–345.
95 N. C. Verma and R. W. Fessenden, Time resolved ESR spectroscopy. IV. Detailed measurement and analysis of the ESR time profile, *J. Chem. Phys.*, 1976, **65**, 2139–2155.
96 I. Draganic, Z. Draganic, L. Petkovic and A. Nikolic, The Radiation Chemistry of Aqueous Solutions of Simple RCN Compounds, *J. Am. Chem. Soc.*, 1973, **95**, 7193–7199.
97 N. Getoff and F. Schworer, Pulsradiolytische bestimmung von geschwindigkeitskonstanten der reaktionen einiger amine mit OH und e_{aq}, *Int. J. Radiat. Phys. Chem.*, 1970, **2**, 81–89.
98 N. Getoff and F. Schworer, Pulse radiolysis of ethyl, n-propyl, n-butyl and n-amyl amine in aqueous solutions, *Int. J. Radiat. Phys. Chem.*, 1973, **5**, 101–111.
99 E. Hayon and M. Simic, Intermediates Produced from the One-Electron Oxidation of Hydrazine. Evidence for the Formation and Decay of Tetrazane and Triazene, *J. Am. Chem. Soc.*, 1972, **94**, 42–47.
100 E. Hayon and M. Simic, Free radical intermediates produced in the pulse radiolysis of simple peptides in aqueous solution, *Intra-Sci. Chem. Rep.*, 1971, **5**, 357.
101 R. H. Bisby, R. B. Cundall and P. Wardman, A pulse radiolysis study of some free radical reactions with erythrocyte membranes, *Biochim. Biophys. Acta*, 1975, **389**, 137–144.
102 P. S. Rao and E. Hayon, Interaction of Hydrated Electrons with the Peptide Linkage, *J. Phys. Chem.*, 1974, **78**, 1193–1196.
103 B. B. Saunders and R. A. Gorse, Reactions of Diethylhydroxylamine with Radiolytically Produced Radicals in Aqueous Solutions, *J. Phys. Chem.*, 1979, **83**, 1696–1701.
104 K. W. Chambers, E. Collinson and F. S. Dainton, Addition of e-aq, H· and ·OH to acrylamide in aqueous solution and reactions of the adducts, *Trans. Faraday Soc.*, 1970, **66**, 142–162.
105 T. H. Tran-Thi, A. Koulkes-Pujo and J. Sutton, Radiolyse des amides et de leurs solutions aqueuses. Journees d' Etude sur la Chimie des Radiations, 1982, pp. 99–102.
106 R. R. H. Farhataziz and E. M. Hansen, Pulse Radiolysis of Liquids at High Pressures. III. Hydrated-Electron Reactions Not Controlled by Diffusion, *J. Chem. Phys.*, 1972, **57**, 2959–2963.
107 S. K. Kapoor and C. Gopinathan, Studies in mixed solvents: Comparison between solvated electron reactions and quenching of excited states, *Int. J. Chem. Kinet.*, 1995, **27**, 535–545.
108 N. S. Fel, P. I. Dolin and V. I. Zolotarevskii, Pulsed radiolysis of formamides, *High Energy Chem.*, 1967, **1**, 132–138.
109 R. Braams, Rate constants of hydrated electron reactions with peptides and proteins, *Radiat. Res.*, 1967, **31**, 8–26.
110 M. Simic and E. Hayon, Interaction of solvated electrons with the amide and imide groups. Acid-base properties of $RC(OH)NH_2$ radicals, *J. Phys. Chem.*, 1973, **77**, 996–1001.
111 B. B. Singh and A. Kabi, Gamma-ray inactivation of trypsin in solution. Effects of various scavengers, *Proc. Natl. Inst. Sci. India, Part B*, 1969, **35**, 291–297.
112 E. Wold, O. Kaalhus, E. S. Johansen and A. T. Ekse, The electron affinity of some radiotherapeutic agents used in cancer therapy, *Int. J. Radiat. Biol. Relat. Stud. Phys., Chem. Med.*, 1980, **38**, 599–611.
113 R. Braams, Rate Constants of Hydrated Electron Reactions with Amino Acids, *Radiat. Res.*, 1966, **27**, 319–329.
114 K. Bobrowski, J. Grodkowski and Z. P. Zagorski, Rate constants of the reactions of tetraalkylammonium cations with e_{aq}^- determined by pulse radiolysis method, *Radiochem. Radioanal. Lett.*, 1979, **40**, 329–337.
115 S. P. Mezyk, Rate constant determination for the reaction of sulfhydryl species with the hydrated electron in aqueous solution, *J. Phys. Chem.*, 1995, **99**, 13970–13975.
116 M. Z. Hoffman and E. Hayon, Pulse Radiolysis Study of Sulfhydryl Compounds in Aqueous Solution, *J. Phys. Chem.*, 1973, **77**, 990–996.
117 S. A. Grachev, E. V. Kropachev, G. I. Litvyakova and S. P. Orlov, Influence of pH on the radiolysis of deaerated aqueous solutions of aminothiols, *Russ. Chem. Bull.*, 1976, **25**, 1248–1253.
118 R. F. Anderson and D. Schulte-Frohlinde, Reactions induced by hydroxyl radical attack on acetylene in aqueous solution. A pulse radiolysis study, *J. Phys. Chem.*, 1978, **1**, 22–26.
119 E. A. Balazs, J. V. Davies, G. O. Phillips and D. S. Scheufele, Polyanions and their complexes. Part III. Reactions of heparin, hyaluronic acid, sodium poly(ethylenesulphonate), sodium poly(styrene-sulphonate), and sodium carboxymethylcellulose with hydroxyl radicals and hydrated electrons, *J. Chem. Soc. C*, 1968, **12**, 1420–1423.
120 L. Engman, J. Lind and G. Merenyi, Redox Properties of Diaryl Chalcogenides and Their Oxides, *J. Phys. Chem.*, 1994, **98**, 3174–3182.

121 T. Sumiyoshi, N. Miura, M. Aikawa and M. Katayama, Pulse Radiolysis Studies on Methyl Methylthiomethyl Sulfoxide in Aqueous Solutions, *Bull. Chem. Soc. Jpn.*, 1982, **55**, 2347–2351.

122 W. Karmann, A. Granzow, G. Meissner and A. Henglein, Die pulsradiolyse einfacher merkaptane in luft freier wassriger losung, *Int. J. Radiat. Phys. Chem.*, 1969, **1**, 395–405.

123 T. Tung and R. R. Kuntz, Hydrated electron reactions with thiols in acidic aqueous solutions, *Radiat. Res.*, 1973, **55**, 256–264.

124 G. G. Jayson, D. A. Stirling and A. J. Swallow, Pulse- and X-radiolysis of 2-mercaptoethanol in aqueous solution, *Int. J. Radiat. Biol. Relat. Stud. Phys., Chem. Med.*, 1971, **19**, 143–156.

125 G. Meissner, A. Henglein and G. Beck, Pulsradiolytische Untersuchung von Dimethylthioather und Dimethylsulfoxyd in waBriger Losung, *Z. Naturforsch., B: Anorg. Chem., Org. Chem., Biochem., Biophys., Biol.*, 1967, **22**, 13–19.

126 M. Z. Hoffman and E. Hayon, One-electron reduction of the disulfide linkage in aqueous solution. Formation, protonation, and decay kinetics of the RSSR- radical, *J. Am. Chem. Soc.*, 1972, **94**, 7950–7957.

127 R. Zhao, J. Lind, G. Merenyi and T. E. Eriksen, Kinetics of one-electron oxidation of thiols and hydrogen abstraction by thiyl radicals from -amino C-H bonds, *J. Am. Chem. Soc.*, 1994, **116**, 12010–12015.

128 W. Roebke, M. Schoneschofer and A. Henglein, Die y-Radiolyse und Pulsradiolyse des Schwefelkohlenstoffs in wabriger Losung, *Z. Naturforsch., B: Anorg. Chem., Org. Chem.*, 1973, **28**, 12–22.

129 G. R. Dey, D. B. Naik, K. Kishore and P. N. Moorthy, Nature of the transient species formed in the pulse radiolysis of some thiourea derivatives, *J. Chem. Soc., Perkin Trans. 2*, 1994, 1625–1629.

130 S. C. Wallace and J. K. Thomas, Reactions in Micellar Systems, *Radiat. Res.*, 1973, **54**, 49–62.

131 K. Asmus, A. Henglein and G. Beck, Pulsradiolytische Untersuchung der Reaktion des hydratisierten Elektrons mit Nitromethan, *Ber. Bunsen-Ges.*, 1966, **70**, 459–466.

132 J. Sutton and T. D. Son, Vitesses de reaction de trois nitroparaffines avec les atomes d'hydrogene et les electrons solvates en milieu aqueux, *J. Chim. Phys.*, 1967, **64**, 688–690.

133 K. P. Madden and H. Taniguchi, An in Situ Radiolysis Time-Resolved Electron Spin Resonance Study of 2-Methyl-2-nitrosopropane Spin Trapping Kinetics, *J. Am. Chem. Soc.*, 1991, **113**, 5541–5547.

134 L. Huang, W. Dong and H. Hou, Investigation of the reactivity of hydrated electron toward perfluorinated carboxylates by laser flash photolysis, *Chem. Phys. Lett.*, 2007, **436**, 124–128.

135 G. V. Buxton, P. G. Ellis and T. F. W. McKillop, Pulse radiolysis study of acrylonitrile in aqueous solution, *J. Chem. Soc., Faraday Trans. 1*, 1979, **75**, 1050–1066.

136 V. Madhavan, N. N. Lichtin and E. Hayon, Protonation Reactions of Electron Adducts of Acrylamide Derivatives. A Pulse Radiolytic-Kinetic Spectrophotometric Study, *J. Org. Chem.*, 1976, **41**, 2320–2326.

137 M. Kumar, M. J. Rao and P. N. Moorthy, Free-radical species from methyl vinyl ketone in aqueous solution: A pulse radiolysis study, *J. Macromol. Sci., Chem.*, 1990, **27**, 299–308.

138 P. N. Moorthy, V. Kumar, K. N. Rao and J. Shankar, Rate constants of reactions of photogenerated solvated electrons with monomers, *Radiat. Eff.*, 1971, **10**, 129–131.

139 V. Madhavan, N. N. Lichtin and E. Hayon, Protonation Reactions of Electron Adducts of Acrylamide Derivatives. A Pulse Radiolytic-Kinetic Spectrophotometric Study, *J. Am. Chem. Soc.*, 1975, **97**, 2989–2995.

140 R. Koester and K. Asmus, Die Reaktionen chlorierter Aethylene mit hydratisierten Elektronen und OH-Radikalen in waessriger Loesung, *Z. Naturforsch., B: Anorg. Chem., Org. Chem., Biochem., Biophys., Biol.*, 1971, **26b**, 1108–1116.

141 D. Behar, R. W. Fessenden and J. P. Hornak, Esr and pulse radiolysis investigation of the radiolysis of sodium vinyl sulfonate, *Radiat. Phys. Chem.*, 1982, **20**, 267–273.

142 Z. D. Draganic, I. G. Draganic and K. Sehested, Radiation Chemistry of Aqueous Solutions of Dicyandiamide, *J. Phys. Chem.*, 1979, **83**, 220–224.

143 M. Kumar and M. H. Rao, Pulse radiolysis study of initiation, dimerization, and propagation steps of 3,3-dimethylacrylic acid in aqueous medium, *J. Macromol. Sci., Chem.*, 1991, **28**, 531–544.

144 A. Safrany and L. Wojnarovits, Radiolysis of hydroxy ethylacrylate in dilute aqueous solutions, *Radiat. Phys. Chem.*, 1993, **41**, 531–537.

145 B. Cercek, Activation energies for reactions of the hydrated electron, *Nature*, 1969, **223**, 491–492.

146 K. W. Chambers, E. Collinson, F. S. Dainton, W. A. Seddon and F. Wilkinson, Pulse radiolysis: Adducts of vinyl compounds and simple free radicals, *Trans. Faraday Soc.*, 1967, **63**, 1699–1711.

147 M. Karelson, *Molecular Descriptors in QSAR/QSPR*, John Wiley & Sons, New York, 2000.

148 J. Shorter, *Correlation Analysis of Organic Reactivity with Particular Reference to Multiple Regression*, John Wiley & Sons, New York, 1982.

149 O. Exner, *Correlation Analysis of Chemical Data*, Plenum Press, New York, 1988.

150 S. Gordon, E. J. Hart and J. K. Thomas, The Ultraviolet Spectra of Transients Produced in the Radiolysis of Aqueous Solutions, *J. Phys. Chem.*, 1964, **68**(5), 1262–1264.

151 S. Gordon, E. J. Hart and J. K. Thomas, The Ultraviolet Spectra of Transients Produced in the Radiolysis of Aqueous Solutions, *J. Phys. Chem.*, 1964, **68**, 1262–1264.

152 L. Eberson, Problems and Prospects of the Concerted dissociative Electron Transfer Mechanism, *Acta Chem. Scand.*, 1999, **53**, 751–764.

153 C. Costentin, M. Robert and J.-M. Saveant, Successive removal of chloride ions from organic polychloride

pollutants. Mechanisms of reductive electrochemical elimination in aliphatic gem-polychlorides, a,b-polychloroalkenes, and a,b-polychloroalkanes in midly protic medium, *J. Am. Chem. Soc.*, 2003, **125**, 10729–10739.

154 M. Z. Hoffman and E. Hayon, Pulse Radiolysis Study of Sulfhydryl Compounds in Aqueous Solution, *J. Phys. Chem.*, 1973, **77**(8), 990–996.

155 C. P. Andrieux, A. Le Gorande and J. M. Saveant, Electron transfer and bond breaking. Examples of passage from a sequential to a concerted mechanism in the electrochemical reductive cleavage of arylmethyl halides, *J. Am. Chem. Soc.*, 1992, **114**, 6892–6904.

156 R. N. Jones and C. Sandorfy, *Chemical Applications of Spectroscopy, Techniques in Organic Chemistry*, Interscience Publishers, New York, N. Y., 1956.

157 C. L. L. Chai, G. A. Heath, P. B. Huleatt and G. A. O'Shea, The first electrochemical study of epidithiopiperazine-2,5-diones, a special class of α,α'-disulfide bridged cyclic dipeptides, *J. Chem. Soc., Perkin Trans. 2*, 1999, 389–392.

158 S. Antonello, R. Benassi, G. Giovanna, F. Taddei and F. Maran, Theoretical and Electrochemical Analysis of Dissociative Electron Transfers Proceeding through Formation of Loose Radical Anion Species: Reduction of Symmetrical and Unsymmetrical Disulfides, *J. Am. Chem. Soc.*, 2002, **124**, 7529–7538.

159 F. Maran, D. D. M. Wayner and M. S. Workentin, Kinetics and mechanism of the dissociative reduction of C-X and X-X bonds (X=O, S), *Adv. Phys. Org. Chem.*, 2001, **36**, 85–166.

160 S. Wang, Q. Yang, F. Chen, J. Sun, K. Luo, F. Yao, X. Wang, D. Wang, X. Li and G. Zeng, Photocatalytic Degradation of Perfluorooctanoic Acid and Perfluorooctane Sulfonate in Water: A Critical Review, *Chem. Eng. J.*, 2017, **328**, 927–942.

161 H. Park, C. D. Vecitis, J. Cheng, W. Choi, B. T. Mader and M. R. Hoffmann, Reductive Defluorination of Aqueous Perfluorinated Alkyl Surfactants: Effects of Ionic Headgroup and Chain Length, *J. Phys. Chem. A*, 2009, **113**, 690–696.

162 W. A. Maza, V. M. Breslin, J. C. Owrutsky, B. B. Pate and A. Epshteyn, Nanosecond Transient Absorption of Hydrated Electrons and Reduction of Linear Perfluoroalkyl Acids and Sulfonates, *Environ. Sci. Technol. Lett.*, 2021, **8**, 525–530.

163 J. Blotevogel, R. J. Giraud and T. Borch, Reductive defluorination of perfluorooctanoic acid by zero-valent iron and zinc: A DFT-based kinetic model, *Chem. Eng. J.*, 2018, **335**, 248–254.

